THETAN BERSERKER: FAST AND STOCHASTIC DISTANCE-BASED CLUSTERING

Anonymous authors
Paper under double-blind review

ABSTRACT

Clustering is a challenging NP-hard problem. Polynomial approximations are of paramount importance for identifying intriguing hidden representations of data at reasonable execution times. In this work, we propose a novel clustering algorithm called Thetan Berserker (TB). TB is a centroid-based clustering method controlled by a single distance parameter. TB revitalizes an old family of sequential algorithms which are adored for their speed but are known to be order sensitive. In addition, TB enables widely used algorithms such as KMeans and DBSCAN by improving their initial conditions. Theoretical aspects are provided in detail along with extensive comparisons and benchmarks. Examples of real world applications are provided using publicly available data of different dimensionalities. A wide range of performance boosts in clustering accuracy, memory usage, and runtime are reported. By dramatically reducing clustering ambiguities, while staying at incredibly low complexity, TB creates a new standard for clustering.

1 INTRODUCTION

Clustering is at the epitome of AI research for more than half a century because when achieved it can infer the underlying structure of the data without any annotations substantially improving automation. It has a range of applications across the fields of science and medicine. For example, collaborative filtering (Ungar & Foster, 1998), trend analysis (Aghabozorgi et al., 2015), LLMs (Tirumala et al., 2023), computer vision (Caron et al., 2018), social networks (Mishra et al., 2007), biological data analysis (Zhao & Karypis, 2005) and signal processing (Orhan et al., 2011). In addition, inference based on clustering is of cardinal importance as it is often applied as the first step in ML pipelines. Information retrieved from clustering is fed into subsequent learning algorithms in many applications such as recommendation systems (Lu et al., 2015), medical analytics (Xu & Wunsch, 2010), and detection of unexpected patterns (Agrawal & Agrawal, 2015).

At the same time clustering still stands as an extremely hard algorithmic problem (NP-hard). Its main challenges include: a) dealing with clustering ambiguity, e.g. clusters mixing, b) tackling order sensitivity i.e. incorrect outputs that depend on data ordering, c) estimating the correct number of clusters, d) long execution times, e) major memory needs, f) large number of hyper-parameters and f) handling of outliers.

Our primary interest to propose a new method stems from the fact that in nature, we often have some prior knowledge of the clusters we intend to find such as the physical dimensions of atoms, cells, animals etc. In such cases, it is much more useful to infer the number of clusters rather than setting a fixed limit on the number of clusters in the data. For this reason we propose a new approach, Thetan Berseker (TB), which uses a single hyper-parameter. Nonetheless, TB outperforms the state-of-the-art in accuracy, speed, and robustness in more than 30 experiments across dimensions and domains.

2 RELATED WORK

Given the wide range of applications, the problem of clustering has been tackled using different approaches such as dimensionality reduction, density estimation, probabilistic methods, spectral methods, and distance-based techniques. Among all these methods, distance-based techniques have been used extensively. Distance-based methods can be separated in four categories. Those that cluster with assumptions concerning: a) the maximum number of clusters (KMeans (Lloyd, 1982), KMeans++ (Arthur & Vassilvitskii, 2007)), Bisecting KMeans (Steinbach & Karypis, 2000; Di &

Gou, 2018), b) a distance threshold (Hierarchical Clustering (HC) (Murtagh & Legendre, 2014)), c) cluster density (MeanShift (Comaniciu & Meer, 2002), DBSCAN (Ester et al., 1996; Schubert et al., 2017)) or d) any combination of the above (HDBSCAN (Campello et al., 2013; McInnes & Healy, 2017)). Another separation can be due to the type of problems that they can try to solve: a) Linearly-separable (KMeans), b) Nonlinearly-separable (DBSCAN) or c) both (Hierachical Clustering). A third divide can be due to the way they process the data: a) sequentially (process each sample as they arrive) or b) offline (process entire dataset).

Researchers have worked to figure out distance-based clustering for linearly separable problems for more than 60 years. The idea that we may be able to approximate clustering solutions started getting attention in the 1950s (due to KMeans) and HC in the 1960s. A few decades after sequential algorithms such the Leader Algorithm (Rush & Russell, 1988), BIRCH (Zhang et al., 1996), BSAS (Theodoridis & Koutroumbas, 2006), MBSAS, TTSAS (Real et al., 2014) and SL (Patra et al., 2011) appeared. In addition, some of these methods such as QuickBundles (Garyfallidis et al., 2012) were successful in specialized domains but not used widely. The reason is that the results of these methods depend heavily on the order of sampling, and therefore results can change drastically from one run to the other. This is known as the ordering problem or order sensitivity. This is not an issue with only sequential algorithms many others including KMeans suffer from this problem.

Thetan Berserker (TB) is introduced here to dramatically reduce this problem while sustaining low complexity at the expense of a single parameter θ. In contrast, BSAS has two parameters, KMeans and MeanShift have three, etc.

In this paper, the focus will be primarily on TB tackling linearly separable problems but TBSCAN will also be introduced that can tackle nonlinear problems. TB will be challenged and compared across 30 experiments and more than 20 methods.

3 THETAN BERSERKER

The name Thetan Berserker (TB) is derived from the way the algorithm works with some inspiration from history. Thetan stems from the algorithm's single distance threshold θ. Berserkers, in the context of this algorithm, are cluster modes that compete for spatial territory in data space.

TB's foundation stone is Thetan Sequential (TS), a straightforward sequential clustering approach. See Alg. 1. TS is in simple terms a simplified version of a basic sequential scheme. In short, TS will visit each data point only once and if a distance metric between a sample and the centroid is less than a threshold θ will enter the same cluster otherwise it will create a new cluster.

TS has multiple advantages: a) single pass - examining each feature only once, b) low time complexity, c) use of a single hyper-parameter, d) minimal memory footprint in contrast for example to Hierarchical Clustering, e) online execution - ideal for asynchronous or streaming systems and f) easy implementation. However, a major disadvantage of TS is the lack of stability when the order of selection changes in datasets with underlying dense clusters (manifestation of the ordering problem).

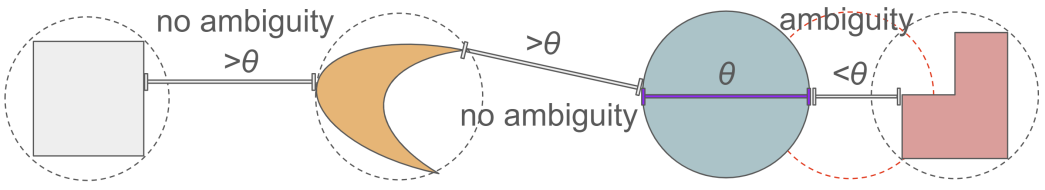

Figure 1: Geometric intuition. Assuming that each shape is filled with 2D points and an L^2 distance threshold matches the diameter of the 3rd shape. Alg. 1 will never mix the first two shapes due to an ordering issue. But it will mix points from the last two shapes. Alg. 2 will be able to separate also the last two without being affected by the ordering problem.

We propose a solution to this problem by studying the space around hypothetical clusters in our data (see Fig. 1). Note that if the closest distance between two points belonging to two different clusters is greater than θ, a single run of TS is sufficient for any ordering due to the clusters being simply said, far enough from each other. But if that is not the case then order sensitivity becomes important.

Definitions. We denote the number of samples $N \in \mathbb{Z}^+$, number of dimensions $D \in \mathbb{Z}^+$. The data sets are denoted with $\boldsymbol{X}$ and contain feature vectors $\boldsymbol{x} \in \mathbb{R}^D$. The Thetan threshold is denoted with $\theta \in \mathbb{R}_{\geq 0}$. The number of clusters is denoted with $K \in \mathbb{Z}^+$. A clustering result is denoted with $\boldsymbol{C}$ and is represented with centroids $\boldsymbol{\mu}$ and labels $\boldsymbol{\lambda}$. $\boldsymbol{C}_\xi$ denotes different clustering number (not individual clusters). In a addition a clustering $\boldsymbol{C}$ contains clusters $c_1, c_2, \ldots, c_K$. For example, $\boldsymbol{C}_2$ means second clustering. But cluster c_3 of $\boldsymbol{C}_2$ has a single centroid $\boldsymbol{\mu}_3$. The description of Thetan Sequential follows (see Alg. 1).

Algorithm 1 Thetan Sequential (TS)

Input: Data $\boldsymbol{X}$ of size $N \times D$ with samples $\boldsymbol{x}_i$, $i \in [0, N-1]$ and hyper-parameter θ
Output: Clustering $\boldsymbol{C}$ of cardinality K with centroids $\boldsymbol{\mu}_k$ and labels Λ

```
x_0 ∈ c_0, K ← 1                                   ▷ First feature starts first cluster
for i = 1 to N − 1 do
    distance_buffer ← infinity[K]                  ▷ Dynamic buffer holds distances from centroids
    for k = 0 to K − 1 do
        d ← distance(x_i, μ_k)                     ▷ This is were metric evaluation takes place
        if d <= θ then
            distance_buffer[k] ← d
    end
    m ← min(distance_buffer)                       ▷ Only the smallest distance is used
    a ← argmin(distance_buffer)
    if m <= θ then
        x_i ∈ c_a                                  ▷ Assign to closest cluster and update centroid
    else
        K ← K + 1                                  ▷ Number of clusters grows
        x_i ∈ c_{K−1}                              ▷ Create a new cluster
    end
end
```

In Thetan Berserker (see Alg. 2), the centroids of TS become an input to a second TS operating directly on these initial centroids. Then this second round of modes (after a low complexity clean-up - relabel function) is brought back to start a second iteration pre-pending the actual data $\boldsymbol{X}$. This is a key point of the innovation. Therefore data which was initially $\boldsymbol{X}$ becomes stack$(\boldsymbol{M}, \boldsymbol{X})$ where $\boldsymbol{M}$ contains previous centroids $\boldsymbol{\mu}_k$, $k \in [0, K-1]$. TB converges very fast and for this purpose, we use only a fixed and small number of iterations (max of 2 is used everywhere in this work).

Algorithm 2 Thetan Berserker (TB)

Input: Data $\boldsymbol{X}$ of size $N \times D$, hyper-parameter θ, *ITER* $= 2$ fixed
Output: Clustering $\boldsymbol{C}$ of cardinality K with centroids $\boldsymbol{\mu}_k$ saved in $\boldsymbol{M}$ of size $K \times D$

```
counter ← 0
repeat
    shuffle(X)                                     ▷ Randomly sample from the data
    if counter = 0 then
        C ← TS(X, θ)                               ▷ TS runs for first time here
    else
        X ← stack(M, X)                            ▷ Previous run centroids are placed in the beginning of X
        C_2 ← TS(X, θ, metric)
        C ← C_2
        X ← destack(X, M)                          ▷ Remove extra Berserker centroids
    end
    C_3 ← TS (M, θ)                                ▷ Cluster only new centroids M
    C ← relabel(C, C_3)                            ▷ Directly update labels providing a new clustering
    counter ← counter + 1
until counter = ITER;
```

Note that exactly the same parameter θ is used across Alg. 1 & 2. The function stack simply prepends the Berserker centroids to data $\boldsymbol{X}$. destack removes these centroids to return the original data $\boldsymbol{X}$. These added and removed centroids are the Berserker centroids because they have survived through a heavily stochastic process (due to the shuffle of the data and the myriad distance pulls). relabel updates the labels Λ of $\boldsymbol{C}$ using $\boldsymbol{C}_3$ results. The size of Λ is N. $\boldsymbol{M}$ of size size $K \times D$ refers to a

matrix containing all centroids $\boldsymbol{\mu}_k$ of clustering $\boldsymbol{C}$. The default number of iterations is fixed to 2. This decision is confirmed by the ablation and iterations study (see Fig. 3).

4 THEORETICAL ASPECTS

We postulate the following theorems assuming L^2 is our norm of choice. First let's identify which datasets would be exactly satisfied (reach a unique and global solution) by Alg. 1.

Theorem 1. Given a clustering problem $\boldsymbol{C}$ with clusters $c_1, c_2, \ldots, c_K$. If there are no pairs of samples $\mathbf{x}_i, \mathbf{x}_j$ from c_i to c_j, $i \neq j$ where $\mathbf{x}_i \in c_i$ and $\mathbf{x}_j \in c_j$, that have a distance $< \theta$, then Alg. 1 will never mix clusters with a threshold parameter θ at exactly one pass. The order of the selection of the samples will have no effect on the final outcome, as long as all features are used.

Proof. In Alg. 1. all the distances are computed either inside a cluster or between clusters. All the inside cluster distances will be $< \theta$ and all the distances between clusters will be $> \theta$. Therefore, there are no cases where clusters are created between the actual clusters given that there are no pairs of samples $\mathbf{x}_i, \mathbf{x}_j$ from cluster i to cluster j that have a distance $< \theta$. ■

This brings us to an equivalence relationship between how the algorithm performs and how close the hypothetical boundaries of the underlying clusters are.

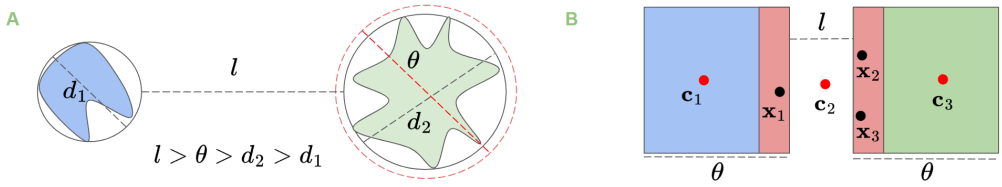

Figure 2: Visual guides. l is the minimum distance between clusters. A) Under the condition above TS will always converge at the global solution in a single pass. Insensitive to order and unaffected by size or geometry (convex vs non-convex). B) Some orders are better than others. TB will resolve the correct clusters even in cases where TS has generated more clusters than necessary (3 shown with blue, red, and green colors rather than 2). Red dots represent TS centroids, black dots represent sampled points near the edges of two uniform distributions.

Lemma 1 If there are no pairs of samples $\boldsymbol{x}_i, \boldsymbol{x}_j$ from cluster c_i to c_j, $i \neq j$ where $\boldsymbol{x}_i \in c_i$ and $\boldsymbol{x}_j \in c_j$ that have a distance $l < \theta$, then due to Theorem 1 the order of selection will not affect the result. However, this also tells us that if the L^2 diameter of the circumscribed hypersphere is $< \theta$ then also the shape of the clusters will not affect the results. In other words, if the contours of the clusters are convex or non-convex the outcome will be the same.

Proof Imagine two clusters c_1 and c_2 bounded (circumscribed) in hyperspheres of diameters d_1 and d_2. Assume that $d_2 > d_1$ (one hypersphere is large than the other one). The clusters can contain any shape of points $\boldsymbol{x}$, convex or non-convex. The minimum distance between c_1 and c_2 is denoted with l. The optimal result would be if Alg. 1 could exactly find the two clusters. Anything more or less that two would be incorrect. Using proof by cases we can see that if $l < d_1, d_2$, and $\theta > d_1, \theta > d_2$ and $\theta > l$. Alg. 1 will not generate two clusters missing the global solution. The same would happen if $l > d_1, d_2$ and $\theta < l$. However, if $l > d_1, d_2$, and $\theta = l$ then Alg. 1 is guaranteed to find the two clusters. This is because all distances between points will be less than threshold θ only in the same clusters. Similarly, we would reach a global solution if $l > d_1, d_2$ and $\theta < l$ but $\theta > d_1, d_2$. In short we now have the following condition where $l > \theta > d_2 > d_1$. In this condition, there is no point $\boldsymbol{x}$ that can be assigned to the wrong cluster. ■.

Although the proof is demonstrated for two clusters, the argument holds for an arbitrary number of clusters. There are specific sizes and interclass distances where the solution is exact, guaranteed, and single pass. Given that clustering is an NP-hard problem with very few theoretically backed ideas we can agree that the fact that TS (Alg. 1) will always provide for these unique data sets for any order of selection is an important observation. Clearly, there are types of datasets that are ideal for TS and some not ideal. For example, those where the underlying clusters are close to each other. This is an area that Alg. 2 (TB) shines.

This is because the nonlinear optimization problem that we are usually trying to solve in centroid/distance-based clustering problems is expressed as $\min_{\mu_1,\ldots,\mu_k,z_{ij}} \sum_{i=1}^{k} \sum_{j=1}^{n} z_{ij} \|\boldsymbol{x}_j -$

$\boldsymbol{\mu}_i\|^2$ subject to $\sum_{i=1}^{k} z_{ij} = 1, \forall j \in \{1, \ldots, n\}$. $z_{ij} = 1$, if $\boldsymbol{x}_j$ is assigned to cluster i or 0 otherwise. KMeans for example is an approximate (heuristic) solution. TS provides a different solution to this nonlinear problem by not using K but a distance threshold θ. Therefore, the assignments are not violated, and still $\sum_{i=1}^{k} z_{ij} = 1, \quad \forall j \in \{1, \ldots, n\}$. However, K is inferred on the go and it can only grow at increments of one, $K \in \{1, \ldots, \infty\}$. Similarly, there is an additional constraint that i (index of data increases monotonically $i \in [1, \ldots, N]$ and stops at a single pass from the data.

Lemma 2 The centroids of a dataset are a reduced representation of the original data. Representing data as their centroids increase empty space (a proxy for sparsity).

Proof Given that the centroids are local averages in an ideal scenario they would exactly approximate the data with one centroid for each sample or one centroid per two or more samples. In that way, we always have a partitioning of the space that is either equal or less than the data. In other words, the centroids are like an infinite shrinkage of the clusters to a point. Moving from one representation to another increases empty space between the clusters. ■

See Fig. 2A for a visual guide. At this stage, it is important to understand that some orders of selection are better than others. Assume for example a grid of uniformly distributed clusters with circumscribed diameters d at equal interclass distances l where $l < d$. We could simply sort the coordinates x, y. That order would be preferred over a random order of selection because the first order would allow Alg. 1 to converge to the global solution in one pass. A random order could generate centroids appearing on empty space between the actual clusters simply because two boundary points could be picked first.

Theorem 2 Starting with the centroids of Alg. 1 helps Alg. 2 reach an improved solution (less incorrectly assigned samples).

Proof We will show this for two uniform distributions at distance l (see visual guide at Fig. 2B). The sides of each distribution is equal to θ. Let's assume that $l < \theta$. A selection order where the first points selected were $\boldsymbol{x}_1, \boldsymbol{x}_2$ and $\boldsymbol{x}_3$ (close to the edges of the two clusters) are guaranteed to create unnecessary extra clusters. This is because Alg. 1 will create a new centroid at $\boldsymbol{\mu} = (\boldsymbol{x}_1 + \boldsymbol{x}_2 + \boldsymbol{x}_3)/3$. However, if we start with $\boldsymbol{c}_1, \boldsymbol{c}_2$ and $\boldsymbol{c}_3$ Alg. 1 is forced to create two enduring centroids $\boldsymbol{\mu}_1 = (\boldsymbol{c}_1 + \boldsymbol{c}_2)/2$ or $\boldsymbol{\mu}_2 = (\boldsymbol{c}_2 + \boldsymbol{c}_3)/2$. Note that the order of selection of centroids (123 or 213 or 312) does not change the outcome. ■

This generalizes for an arbitrary number of clusters. See details at section A.12. Due to Theorems 1-2 and Lemmas 1-2, TB is adding a new constraint that TS cannot satisfy. The constraint is $\|\boldsymbol{\mu}_i - \boldsymbol{\mu}_i\| > \theta$. Centroids will be far from each other providing better coverage and a reduced to number of clusters.

Complexity analysis. Alg. 1 has a worst-case time complexity (upper bound) $\mathcal{O}(NKD)$ that depends on the number of samples N and the number of estimated clusters K and number of dimensions D. We assume here that most of the computation is from the calculation of distances between samples and centroids. The worst case complexity takes place when every data point belongs to a different cluster (all singleton clusters). In such an event the worst time complexity is $\mathcal{O}(DN^2)$. The best time complexity is $\mathcal{O}(ND)$ when only one cluster. Assuming most memory is spent on saving centroids and labels, Alg. 1 has a best case (lower bound) space complexity of $\mathcal{O}(N)$ and worst case (upper bound) of $\mathcal{O}(N)$. The highest bound is when all clusters are singleton clusters. However, in most cases $K << N$. Therefore, TS requires a remarkably small amount of memory. TB (Alg. 2) builds on top of TS (Alg. 1) but now the time complexity also depends on the number of iterations I. However, everywhere in this work we fixed $I = 2$. Therefore, Alg. 2 is of the same complexity as Alg. 1. In addition, TB's cleanup operations work on the space of centroids or small label updates. Therefore, they do not change the order of complexity. In short, TB's time and space complexity is the same as that of TS. This is also experimentally shown in Tab. 1. Proofs available at A.8 and A.9.

Other algorithmic contributions: I) In order to compare TB, we introduce a simple iterative version of TS. TSR (Thetan Sequential Randomized) is a version where we simply run TS multiple times (default 10) for different shuffles of the data, collect all their centroids, re-cluster them, and reassign the data to the last round of centroids. II) In order to increase our understanding of the differences between BSAS and KMeans, we introduced a new algorithm TBK (TB seeding + KMeans) which starts with TB and then get the centroids of the K biggest clusters and provide them as initialization for KMeans. This is a task of improving KMeans seeding. III) Because TS and TB are primarily focused

Table 1: Comparisons between clustering algorithms. Highlight identifies top performers.

	Method	AC ↑		NMI ↑		SIL ↑		FMS ↑		ARS ↑		Clusters		Runtime ↓		Memory ↓	
		mean	std	mean	std	mean	std	mean	std	mean	std	mean	std	mean	std	mean	std
1	BIRCH	0.571	0.057	0.956	0.004	0.509	0.008	0.872	0.015	0.871	0.015	296.0	5.8	7.518	0.103	5.400	0.516
2	BSAS	0.155	0.020	0.949	0.003	0.502	0.008	0.857	0.012	0.857	0.012	300.0	0.0	5.999	0.065	155.000	0.000
3	CLARANS	0.012	0.008	0.877	0.003	0.282	0.008	0.574	0.010	0.568	0.010	300.0	0.0	5726.562	1632.025	27.000	0.000
4	CURE	0.814	0.026	0.964	0.001	0.542	0.001	0.920	0.002	0.919	0.002	300.0	0.0	2518.961	375.720	174.000	0.000
5	EM_GMM	0.931	0.008	0.971	0.001	0.536	0.002	0.927	0.003	0.927	0.003	300.0	0.0	138.870	9.507	1375.000	0.000
6	FCM	0.131	0.024	0.922	0.002	0.403	0.004	0.703	0.005	0.698	0.006	300.0	0.0	1014.085	366.602	3091.000	0.000
7	MBSAS	0.152	0.019	0.949	0.003	0.502	0.008	0.858	0.012	0.857	0.012	300.0	0.0	6.692	0.120	155.000	0.000
8	OPTICS	0.786	0.066	0.300	0.030	-0.628	0.027	0.067	0.001	0.003	0.000	63.3	5.8	739.002	94.169	188.000	0.000
9	TB	0.997	0.002	0.976	0.000	0.556	0.001	0.953	0.001	0.953	0.001	300.9	0.7	0.349	0.005	8.000	0.000
10	TBK	1.000	0.000	0.976	0.000	0.556	0.001	0.954	0.001	0.954	0.001	300.0	0.0	0.869	0.008	8.000	0.000
11	TS	0.862	0.023	0.971	0.001	0.530	0.005	0.938	0.004	0.937	0.004	320.7	4.3	0.161	0.002	1.000	0.000
12	TSR	0.994	0.005	0.976	0.001	0.555	0.001	0.953	0.001	0.953	0.001	301.5	1.4	7.829	0.056	4.000	0.000
13	TTSAS	0.145	0.027	0.949	0.004	0.482	0.014	0.861	0.014	0.861	0.014	318.7	5.6	6.444	0.127	156.000	0.000
14	BISECTING	0.218	0.014	0.931	0.000	0.436	0.002	0.778	0.001	0.776	0.001	300.0	0.0	0.787	0.030	13.000	0.000
15	DBSCAN	0.825	0.014	0.722	0.002	0.100	0.004	0.083	0.001	0.019	0.000	301.0	0.8	1.355	0.016	26.100	0.316
16	HDBSCAN	1.000	0.001	0.887	0.001	0.414	0.002	0.295	0.003	0.195	0.003	300.0	0.0	132.364	3.192	184.000	0.000
17	KMEANS	0.522	0.075	0.945	0.006	0.478	0.015	0.818	0.026	0.817	0.027	300.0	0.0	2.394	0.229	8.400	0.516
18	KMEANS++	0.855	0.035	0.968	0.002	0.535	0.005	0.919	0.009	0.919	0.009	300.0	0.0	2.921	0.215	20.000	0.000
19	KMEDIANS	0.104	0.014	0.942	0.003	0.478	0.008	0.820	0.013	0.819	0.013	300.0	0.0	31.176	0.241	506.000	0.000
20	MEANSHIFT	0.999	0.002	0.976	0.001	0.556	0.001	0.954	0.002	0.953	0.002	299.9	0.3	1014.352	23.430	37.300	1.418
21	MEANSHIFT++	0.033	0.009	0.720	0.000	0.312	0.003	0.291	0.000	0.166	0.000	33.1	0.3	3.802	0.059	8.000	0.000
22	XMEANS	0.591	0.037	0.951	0.003	0.494	0.007	0.846	0.012	0.845	0.013	300.0	0.0	76.938	4.836	158.000	0.000
23	TBSCAN	0.997	0.003	0.975	0.000	0.555	0.001	0.953	0.001	0.953	0.001	300.8	1.0	3.320	0.019	8.000	0.000

on linearly separable problems we introduce an algorithm to deal with density-based nonlinear clustering problems. We call this algorithm TBSCAN. Basically, we start with TB and then the output centroids become input to a modified DBSCAN version (with additional parameters epsilon and min_samples to control for nonlinear shapes). In summary, we introduce 1 major algorithm TB, and 4 supporting (TS, TSR, TBK, and TBSCAN). Extensive comparisons follow.

5 RESULTS

All results were performed on a single thread of a single CPU. No GPUs were used in this work. We compare our methods with other well known clustering methods. Various metrics are used for evaluation including Normalized Mutual Information (NMI), Silhouette score (SIL), Fowlkes-Mallows Score (FMS), and Adjusted Rand Score (ARS). Because clustering evaluation can often be ambiguous we also introduce a stricter metric Apparent Centroid distance (AC) (see details in A.1). All experiments, including the compared methods and the evaluation, were done using scikit-learn (Pedregosa et al., 2011), pyclustering (Novikov, 2019), meanshift++ (directly from author's GitHub) and skfuzzy packages (for fuzzy-cmeans). Tracemalloc module was used to measure peak memory. Runtime was reported with Python's time package. The Thetan methods were developed in C (via Cython). All methods have underlying C or C++ implementations via Pythonic interfaces. Due to the large number of experiments most of the results and details are available in Appendix A.

5.1 SIMULATION EXPERIMENTS

We randomly sample from multi-variate normal distributions with mean 0 and identity covariance matrix. Each distribution contains 500 samples. The centers of the distributions are set on a 30×10 grid. Therefore, we have a total of 300 ground truth clusters. Each distribution center is at a distance of 5 units from its closest neighboring center. This creates a dense clustering setting which will be challenging for most algorithms. The total number of points (samples) in this experiment is $150,000$. **Ablation Study**. In Fig. 3A, we use the setup above to study if the different parts of TB algorithm are actually improving overall accuracy. As Alg. 2 suggests, TB is split into 4 parts: I) TS, II) CL, III) TS2, and IV) CL2, where TS stands for Thetan Sequential and CL stands for cluster new centroids and update labels. The experiment was repeated 20 times. As we can see in boxplots of Fig. 3A every part of the algorithm clearly improves overall accuracy. **Convergence Study**. In Fig. 3B we examine the hypothesis saying that TB may need only two iterations. In this experiment, we check if repeating iterations can actually improve the results. As shown in the violin plot of Fig. 3B repeating TB iterations does not improve NMI scores. TB01 is the default version with 2 iterations. The experiment goes up to TB14 which has 15 iterations. The statistics shown are from 20 repetitions. In short, TB does convergence in only 2 iterations for the experiment at hand. **Inter-class distance trade-off**. In this experiment, we study how algorithms perform as the inter-clusters distances shrink or grow. See Fig. 3C. Here the minimum distances across two clusters change from 3 to 10. As expected all methods have trouble when the distances between clusters are small and that gradually improves as

the distances grow. The parameters used are: TB (θ 3.6), HDBSCAN (min_samples 40), KMeans++ (K 300, tol. 0.0001), and MeanShift (bandwidth 2.6).

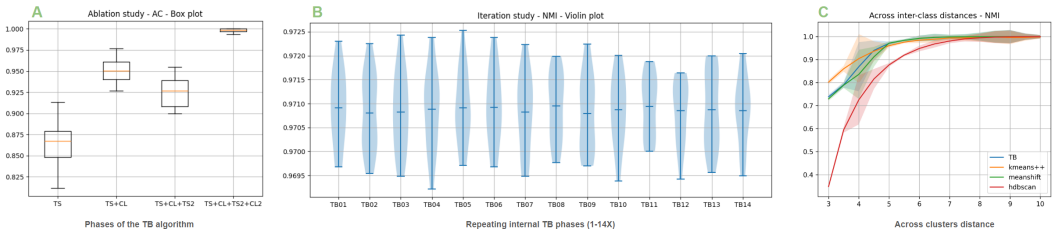

Figure 3: Study of trade-offs. A) Ablation study shows that all parts of TB contribute to its performance. B) Iteration study shows fast convergence. C) NMI improves as clusters become more distant from each other.

Large comparisons. We evaluated more than 20 methods in clustering the 300 clusters as described above. All parameters used are at section A.3 The statistics shown are after 10 repetitions for each method. Results are summarized on Tab. 1 and Fig. A2-A3. Thetan Berserker (TB) is one of the best performing methods. TS is only 2X faster than TB but it identifies the wrong number of clusters and has low evaluation scores. HDBSCAN generates comparable scores (AC) but is 200X slower. KMeans++ takes 4X more time but makes estimation mistakes. MeanShift takes a lot longer, 1000X more time. DBSCAN is only 2X slower than TB. However, it does not achieve high evaluation scores. Therefore, we consider TB to perform well for such datasets. In addition, TSR has higher scores that TS but it generates a less accurate number of clusters than TB. TBK outperforms KMeans++ (stands for KMeans with KMeans++ seeding (Arthur & Vassilvitskii, 2007)). TBSCAN is faster than HDBSCAN by 48X. BSAS, MBSAS, TTSAS, and BIRCH lose accuracy across many evaluation metrics. In contrast, TB has a unique performance balancing memory, runtime, and accuracy. Visual plots are available in Fig. A4-A15. TB continued performing at the highest level in experiments with outliers and uniform distributions of equal or varying scales (see Fig. A33- A33).

Predicting θ. TB has only one parameter while most of the methods have at least two or three parameters. Nonetheless, two important questions emerge: a) Would it be possible to find θ automatically from the data? b) How fast? Finding θ often depends on what someone wants to do and therefore it cannot always be found automatically. However, apart from established techniques such as the Elbow method (Liu & Deng, 2021) researchers can use random walks effectively. In more detail, by storing the distances between consecutive points we can create a footprint of the dataset. This is shown in Fig. 4A. The distributions of the random walks can regress the distance across clusters. This is a method that is highly efficient ($\mathcal{O}$(ND)). Note that each distribution is clearly distinguishable from another. Here the minimum interclass distance is from 5 to 45 units. Other more advanced methods include the Auto Elbow Method (Onumanyi et al., 2022), Gap Statistic (Tibshirani et al., 2001) and maximizing the Silhouette Score (Rousseeuw, 1987) but they require a larger number of samples.

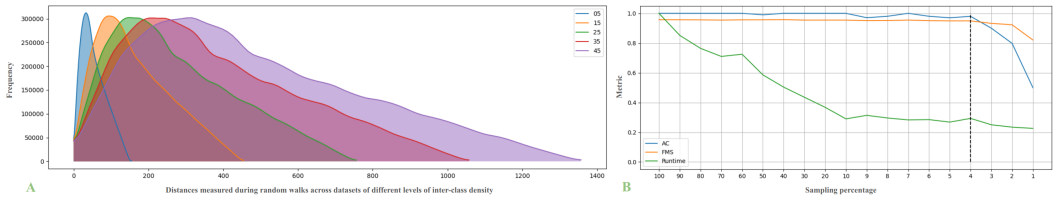

Figure 4: Predicting θ and sub-sampling. A) Linear-time random walks can be used to infer good estimates for hyper-parameter θ. Here showing distributions for growing inter-class distances of 5, 15, 25, 35, and 45 units. A pattern emerges. B) TB seems robust in sampling parts of the data. Here we sample from 100% down to 1%. Accuracy stays high until after 4% while runtime is reduced. This is evidence of robustness. Runtime is normalized by dividing with an initial runtime of 83ms at 100%.

Robustness in sub-sampling. Another important way to measure robustness of an algorithm is to see how stable it can be while reducing the actual data. In this experiment, we start with the same setup as in the previous section but now we measure accuracy after keeping from 100% down to 1% of the data. See Fig. 4. Samples are removed randomly. Accuracy measured by AC metric stays high until after 4% while runtime is reduced because less data are being used. Runtime is normalized to fit

the plot by dividing with an initial runtime of 83ms. Holding AC after removing 96% (100-4) of the data is strong evidence of robustness to large density changes.

5.2 Standardized Benchmarks

The widely used and publicly available clustering benchmarks framework (Gagolewski, 2022) is applied here. Eight linearly and eight nonlinearly-separable datasets have been processed using TB and TBSCAN respectively. As seen on Tab. A1, TB achieves high clustering performance on linearly separable datasets with minimal runtime, while TBSCAN shows overall high accuracy on non-linear datasets. Parameters used are reported on Tab. A4. For this evaluation, we used the 2D embedding of the digits dataset from scikit-learn (Pedregosa et al., 2011) which consists of 1,797 samples, each with 64 features. Tab. A3 presents a comparison of various clustering methods, with TB emerging as the most efficient in terms of both runtime and peak memory usage. TB achieves the lowest runtime (0.0008s) and requires no additional memory (<1 MB), making it highly resource-efficient compared to the hierarchical clustering (HC) methods. While HC-WARD outperforms TB slightly in terms of clustering accuracy metrics like RI (0.90499) and ARI (0.51293), TB maintains competitive performance with respectable values across NCA (0.52226), RI (0.84255), and ARI (0.37490). Given its efficiency, TB offers a significant advantage in scenarios where resource constraints are critical, while still delivering comparable clustering quality.

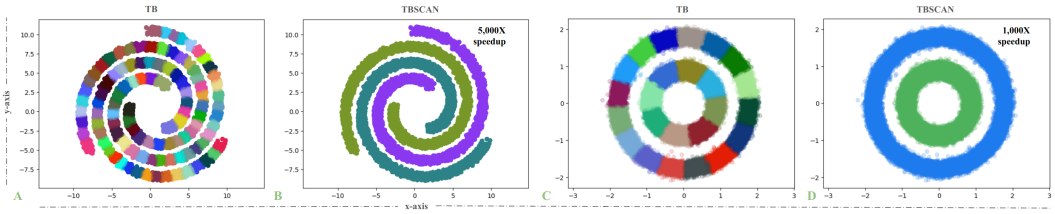

Figure 5: TB enables density based approaches for nonlinearly-separable problems. Here shown with Spiral and Circles benchmarks. TB reads the x,y coordinates in a completely random fashion, but it is still able to evenly separate the clusters (A, C). TBSCAN is up to 5,000X faster than DBSCAN (B, D).

Nonlinearly-separable benchmarks. In this experiment, we used the benchmarks Spiral and Circles from Scikit-Learn. We increased the numbers of points of the datasets to go up to the level of hundreds of thousands. The purpose of this experiment is to examine the behavior of TB and TBSCAN on testbed nonlinear datasets. In Fig. 5, we see that TB is building equivariant parts and then TBSCAN connects them to build the nonlinear parts. For the Spiral dataset, we used TB (θ 1.0) and TBSCAN (eps 0.5, min_samples 1). Number of points 375,000. For the Circles dataset (1 million points) we used TB (θ 1.0) and TBSCAN (eps 0.8, min_samples 1).

6 Applications

6.1 Superpixels

Here we examine if TB can assist superpixel segmentation. NYUV2(Arbelaez et al., 2011) and BSDS500(Nathan Silberman & Fergus, 2012) datasets are used. Fig. 6 shows qualitative results. For TB, we assign the 2D spatial information and pixel intensity as features of each pixel for clustering. Felzenszwalbs' method (Felzenszwalb & Huttenlocher, 2004), SLIC(Achanta et al., 2012), Quickshift(Vedaldi & Soatto, 2008) and Compact watershed(Neubert & Protzel, 2014) were selected as a comparison method mainly for their availability. Despite the fact that our method is not tailored for superpixel purposes, it creates object boundary compliant superpixels compared to other methods. All methods excluding TB were run using scikit-image(van der Walt et al., 2014), with the following parameters: 1. BSDS500 dataset: scale 300, sigma 1.0, minimum size 30 for Felzenszwalbs's method, number of segments 200, compactness 0.1, sigma 1 with automatic parameter estimation for SLIC, kernel size 7, maximum distance 30, ratio 0.5 for Quickshift and markers 125, compactness 0.00001 for Compact Watershed and θ 0.17 for TB. NYUV2 dataset: scale 75, sigma 1.0, minimum size 30 for Felzenszwalbs's method, number of segments 400, compactness 0.1, sigma 1 with automatic parameter estimation for SLIC, kernel size 5, maximum distance 30, ratio 0.5 for Quickshift and markers 200, compactness 0.00001 for Compact Watershed. For TB θ 0.19. Grid search with qualitative evaluation was used to select the optimal parameters. The input to TB was simply an array

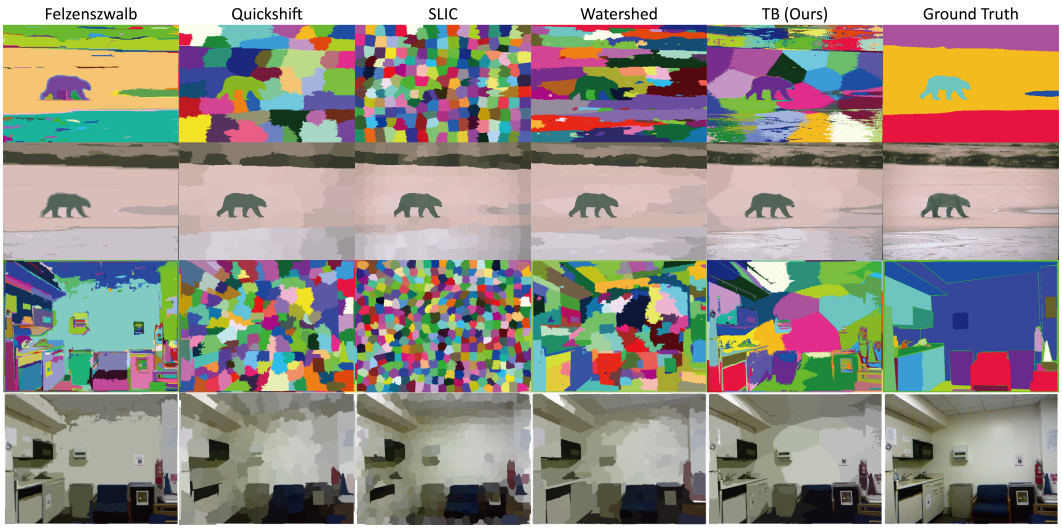

Figure 6: Example results from the BSD500 (top two rows) and the NYUV2 (bottom two rows) datasets.

X holding the normalized position (x, y) and LAB space intensity features (weighted to balance between spatial information) for each pixel in the image. Details are shown on Tab. 2. We calculate metrics suggested by Stutz et al. (2018). More specifically, the table contains scores for Boundary Recall (REC) (Martin et al., 2004), Normalized Undersegmentation Error and its variant (UE, UEB) (Van den Bergh et al., 2015; Neubert & Protzel, 2012), Explained Variation (EV) (Moore et al., 2008) and Compactness (CO) (Schick et al., 2012). Higher REC, EV, CO, and lower UE, UEB indicate more appropriate superpixels. Runtime and the number of superpixels are indicated in the table as well. As the BSDS500 dataset has multiple ground truth labels, the metric on each ground truth was averaged first, before averaging the results of all images in the dataset. In both datasets, TB is capable of creating superpixels of reasonable quality, and high average metrics. We want to emphasize that no further processing was done to modify the method to be superpixel friendly (e.g. smoothing kernels, connectivity regularizations). High metrics on the BSDS500, which had multiple ground truths, also suggest our method is capable of creating superpixels that are generalizable between different goals.

Table 2: Comparisons between TB and superpixel algorithms.

Datasets	Algorithms	REC ↑		UEB ↓		UE ↓		EV ↑		CO ↑		Superpixels		runtime (sec) ↓	
		mean	std	mean	std	mean	std	mean	std	mean	std	mean	std	mean	std
BSDS500	Felzenszwalbs	0.420	0.091	0.969	0.0135	0.225	0.340	0.0506	0.0324	**2.44e-03**	6.43e-03	112	47.3	0.147	5.75e-03
	SLIC	0.271	0.0592	0.980	8.06e-03	**0.0112**	0.0103	0.0648	0.0305	1.53e-05	1.06e-06	186	1.29	0.164	3.41e-03
	Quickshift	0.291	0.0903	0.979	0.0103	0.0728	0.0854	0.0569	0.0309	2.63e-04	1.26e-04	39	6.39	3.64	0.0782
	Compact Watershed	0.316	0.0829	0.977	0.0101	0.0565	0.0580	0.0566	0.0313	1.35e-04	4.01e-05	126	0.00	**0.0736**	4.55e-03
	TB (Ours)	**0.745**	0.0972	**0.944**	0.0222	0.0344	0.0326	**0.0811**	0.0300	1.27e-05	2.26e-05	87.6	21.0	0.388	0.0642
NYUV2	Felzenszwalbs	**0.540**	0.0593	**0.929**	0.0175	1.41e-03	1.73e-03	0.0824	0.0159	**5.18e-05**	7.69e-05	580	178	0.334	0.0228
	SLIC	0.193	0.0212	0.975	6.69e-03	2.23e-04	1.56e-04	0.0712	0.0168	3.56e-06	1.31e-07	388	2.36	0.338	6.71e-03
	Quickshift	0.233	0.0349	0.970	7.93e-03	**1.92e-04**	1.76e-04	0.0756	0.0150	1.98e-05	4.67e-06	169	19.0	3.99	0.0647
	Compact Watershed	0.242	0.0396	0.968	8.49e-03	2.78e-04	2.15e-04	0.0736	0.0160	4.37e-05	9.47e-06	192	0.00	**0.154**	7.28e-03
	TB (Ours)	0.445	0.0800	0.941	0.0200	8.20e-04	6.60e-04	**0.0872**	0.0164	2.24e-05	2.07e-05	74.2	12.5	0.687	0.0942

6.2 Processing 3D brains

We examined if TB would be affected by the 3D structure of the brain. Here we used T1 images from HCP (Van Essen et al., 2013) containing 1,200 subjects which are widely common in MR experiments. These images can have millions of voxels and intricate underlying anatomy. HCP has multi-modal neuroimaging and behavioral data of young adult subjects aged 22-35 at 3 Tesla (3T). Dimensions are $260 \times 311 \times 260$ with a voxel resolution of 0.7 mm^3. The features used are the x, y, z scanner coordinates of each voxel and intensity w of the image. To balance the features we multiplied the ws by 3. Therefore, matrix X is now a 2D array of shape 21,023,600 $\times 4$. θ value is 150. In Fig. 7 we see the results of this experiment. TB takes only on average 17.38 seconds to cluster this dataset. The clustering labels match well with the underlying anatomy (A-C). In addition, we built a new image from the labels where each voxel is replaced with its corresponding centroid w value (B). The results match the original anatomy without blurring the edges. Notably, a single label

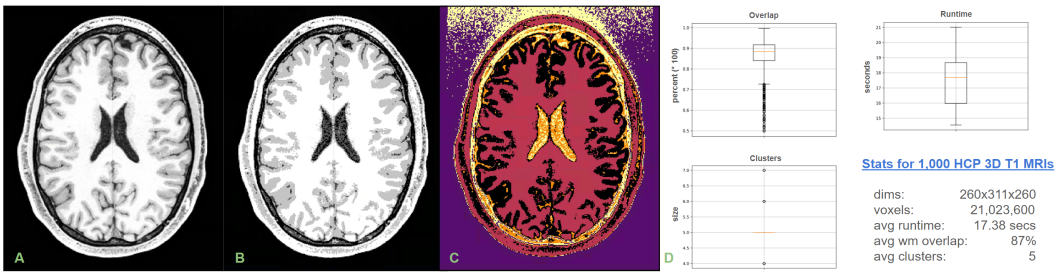

Figure 7: TB processing 1,000 3D brain images (θ150). A) Original HCP data, subject 102008, b) Reconstructed image of the same from TB output (contains only 5 unique intensity values), c) Clusters found (5 clusters), D) Statistical analysis and summary for all participants. TB consistently produces 5 clusters keeping the white matter solid (87% overlap). Each image contains 21 million voxels and clustered in 17.38 sec (avg).

is used for most of the white matter. The experiment shows that TB can process millions of features in seconds providing meaningful results. The compression ratio achieved is 26.6X. 160MB (original size), 147 MB (GZip) and 6 MB (GZip after TB). More details, including results at different θ and comparisons against other methods are available at section A.19 (see Fig. A45).

6.3 Pattern recognition in time and high dimensions

A series of experiments studying the ability of TB to find repeating patterns in familiar signals and real publicly available ECG data (Wagner et al., 2020) is reported at section A.5. TB shows a striking ability to find all sorts of patterns in the data unaffected be artifacts and noise as shown in section A.21. Another important experiment is to see how TB performs with high dimensional data. For this purpose we used 100 thousand text embeddings with 1024 dimensions from Hugging Face see details in section A.20. TB was able to achieve the highest scores while using the least amount of memory.

7 Discussion

In this work, a new algorithmic set around Thetan Berserker (TB) was introduced. TB demonstrates an important advantage both in speed and memory use. In addition, TB shows an increase in accuracy across many evaluation metrics, simulations, benchmarks, and real data experiments. Another surprising fact about TB is that it is able to provide highly accurate low level segmentation. This is indeed surprising because we simply provided the location and intensity of each pixel as input. Usually, superpixel algorithms are specifically tailored for superpixel problems and highly optimized for that specific purpose. However, TB does not have this requirement nor was it built for that task in mind. Nonetheless, it generates useful superpixels at acceptable times. More importantly, the results match well the underlying images simplifying the underlying representations in a meaningful manner . Similarly, we achieve great overall segmentations for 3D imaging data. Both types of data are remarkably hard to process. Nonetheless, TB identifies the relevant structures in the data without compromising edges which achieving a outstanding compression ratio (see Fig. 7). However, TB is also anticipated to struggle with the curse of dimensionality as any other clustering method. We were happy to report results in grouping text embedding of up to 1024 dimensions. TB is not bound by density limits in the same way that MeanShift, HDBSCAN, and DBSCAN do as distributions become sparser when dimensions increase. It is also not bound to be affected by outliers as KMeans. TB outperformed KMeans++ seeding. TB is still aimed for linearly separable clusters and it will not perform well on nonlinearly separable clustering problems. In these cases, TBSCAN should be used instead (see Tab. A3). The proposed approach is general purpose and can be used across data science. More importantly, it provides some theoretical ground for the AI community to rethink and rework unsupervised learning. The code will be available on GitHub upon acceptance for publication.

8 Conclusion

Thetan Berserker (TB) is as uniquely accurate as fast clustering algorithm. In addition, TB enables widely used algorithms by improving their conditioning and initialization. Important real-world applications were demonstrated such as segmentation of natural images, edge-preserving compression of magnetic resonance data and grouping of text embeddings. TB outperformed more than 20 methods across 30 experiments.

REFERENCES

Radhakrishna Achanta, Appu Shaji, Kevin Smith, Aurelien Lucchi, Pascal Fua, and Sabine Süsstrunk. Slic superpixels compared to state-of-the-art superpixel methods. *IEEE transactions on pattern analysis and machine intelligence*, 34(11):2274–2282, 2012.

Saeed Aghabozorgi, Ali Seyed Shirkhorshidi, and Teh Ying Wah. Time-series clustering–a decade review. *Information Systems*, 53:16–38, 2015.

Shikha Agrawal and Jitendra Agrawal. Survey on anomaly detection using data mining techniques. *Procedia Computer Science*, 60:708–713, 2015.

Mihael Ankerst, Markus M Breunig, Hans-Peter Kriegel, and Jörg Sander. Optics: Ordering points to identify the clustering structure. *ACM Sigmod record*, 28(2):49–60, 1999.

Pablo Arbelaez, Michael Maire, Charless Fowlkes, and Jitendra Malik. Contour detection and hierarchical image segmentation. *IEEE Trans. Pattern Anal. Mach. Intell.*, 33(5):898–916, May 2011. ISSN 0162-8828. doi: 10.1109/TPAMI.2010.161. URL http://dx.doi.org/10.1109/TPAMI.2010.161.

David Arthur and Sergei Vassilvitskii. k-means++: the advantages of careful seeding. In *Proceedings of the Eighteenth Annual ACM-SIAM Symposium on Discrete Algorithms*, SODA '07, pp. 1027–1035, USA, 2007. Society for Industrial and Applied Mathematics. ISBN 9780898716245.

James C Bezdek, Robert Ehrlich, and William Full. Fcm: The fuzzy c-means clustering algorithm. *Computers & geosciences*, 10(2-3):191–203, 1984.

Ricardo JGB Campello, Davoud Moulavi, and Jörg Sander. Density-based clustering based on hierarchical density estimates. In *Pacific-Asia conference on knowledge discovery and data mining*, pp. 160–172. Springer, 2013.

Mathilde Caron, Piotr Bojanowski, Armand Joulin, and Matthijs Douze. Deep clustering for unsupervised learning of visual features. In *Proceedings of the European Conference on Computer Vision (ECCV)*, pp. 132–149, 2018.

Dorin Comaniciu and Peter Meer. Mean shift: A robust approach toward feature space analysis. *IEEE Transactions on pattern analysis and machine intelligence*, 24(5):603–619, 2002.

Jian Di and Xinyue Gou. Bisecting k-means algorithm based on k-valued selfdetermining and clustering center optimization. *J. Comput.*, 13(6):588–595, 2018.

Jiangyong Duan and Lili Guo. Variable-length subsequence clustering in time series. *IEEE Transactions on Knowledge and Data Engineering*, 34(2):983–995, 2022. doi: 10.1109/TKDE.2020.2986965.

Delbert Dueck. *Affinity propagation: clustering data by passing messages*. University of Toronto Toronto, ON, Canada, 2009.

Martin Ester, Hans-Peter Kriegel, Jörg Sander, Xiaowei Xu, et al. A density-based algorithm for discovering clusters in large spatial databases with noise. In *Kdd*, volume 96(34), pp. 226–231, 1996.

Pedro F Felzenszwalb and Daniel P Huttenlocher. Efficient graph-based image segmentation. *International journal of computer vision*, 59:167–181, 2004.

Marek Gagolewski. A framework for benchmarking clustering algorithms. *SoftwareX*, 20:101270, 2022. ISSN 2352-7110. doi: https://doi.org/10.1016/j.softx.2022.101270. URL https://www.sciencedirect.com/science/article/pii/S2352711022001881.

Eleftherios Garyfallidis, Matthew Brett, Marta Morgado Correia, Guy B Williams, and Ian Nimmo-Smith. Quickbundles, a method for tractography simplification. *Frontiers in neuroscience*, 6:175, 2012.

Sudipto Guha, Rajeev Rastogi, and Kyuseok Shim. Cure: An efficient clustering algorithm for large databases. *ACM Sigmod record*, 27(2):73–84, 1998.

Fan Liu and Yong Deng. Determine the number of unknown targets in open world based on elbow method. *IEEE Transactions on Fuzzy Systems*, 29(5):986–995, May 2021. ISSN 1941-0034. doi: 10.1109/TFUZZ.2020.2966182.

Stuart Lloyd. Least squares quantization in pcm. *IEEE transactions on information theory*, 28(2): 129–137, 1982.

Jie Lu, Dianshuang Wu, Mingsong Mao, Wei Wang, and Guangquan Zhang. Recommender system application developments: a survey. *Decision Support Systems*, 74:12–32, 2015.

Nicos Maglaveras, Telemachos Stamkopoulos, Konstantinos Diamantaras, Costas Pappas, and Michael Strintzis. Ecg pattern recognition and classification using non-linear transformations and neural networks: A review. *International journal of medical informatics*, 52(1-3):191–208, 1998.

David R Martin, Charless C Fowlkes, and Jitendra Malik. Learning to detect natural image boundaries using local brightness, color, and texture cues. *IEEE transactions on pattern analysis and machine intelligence*, 26(5):530–549, 2004.

Leland McInnes and John Healy. Accelerated hierarchical density based clustering. In *2017 IEEE international conference on data mining workshops (ICDMW)*, pp. 33–42. IEEE, 2017.

Nina Mishra, Robert Schreiber, Isabelle Stanton, and Robert E Tarjan. Clustering social networks. In *International Workshop on Algorithms and Models for the Web-Graph*, pp. 56–67. Springer, 2007.

T.K. Moon. The expectation-maximization algorithm. *IEEE Signal Processing Magazine*, 13(6): 47–60, 1996. doi: 10.1109/79.543975.

Alastair P Moore, Simon JD Prince, Jonathan Warrell, Umar Mohammed, and Graham Jones. Superpixel lattices. In *2008 IEEE conference on computer vision and pattern recognition*, pp. 1–8. IEEE, 2008.

Kasper Overgaard Mortensen, Fatemeh Zardbani, Mohammad Ahsanul Haque, Steinn Ymir Agustsson, Davide Mottin, Philip Hofmann, and Panagiotis Karras. Marigold: Efficient k-means clustering in high dimensions. *Proc. VLDB Endow.*, 16(7):1740–1748, March 2023. ISSN 2150-8097. doi: 10.14778/3587136.3587147. URL https://doi.org/10.14778/3587136.3587147.

Michal Moshkovitz, Sanjoy Dasgupta, Cyrus Rashtchian, and Nave Frost. Explainable k-means and k-medians clustering. In *International conference on machine learning*, pp. 7055–7065. PMLR, 2020a.

Michal Moshkovitz, Sanjoy Dasgupta, Cyrus Rashtchian, and Nave Frost. Explainable k-means and k-medians clustering. In Hal Daumé III and Aarti Singh (eds.), *Proceedings of the 37th International Conference on Machine Learning*, volume 119 of *Proceedings of Machine Learning Research*, pp. 7055–7065. PMLR, 13–18 Jul 2020b. URL https://proceedings.mlr.press/v119/moshkovitz20a.html.

Fionn Murtagh and Pierre Legendre. Ward's hierarchical agglomerative clustering method: which algorithms implement ward's criterion? *Journal of classification*, 31:274–295, 2014.

Pushmeet Kohli Nathan Silberman, Derek Hoiem and Rob Fergus. Indoor segmentation and support inference from rgbd images. In *ECCV*, 2012.

Peer Neubert and Peter Protzel. Superpixel benchmark and comparison. In *Proc. Forum Bildverarbeitung*, volume 6, pp. 1–12, 2012.

Peer Neubert and Peter Protzel. Compact watershed and preemptive slic: On improving trade-offs of superpixel segmentation algorithms. In *2014 22nd international conference on pattern recognition*, pp. 996–1001. IEEE, 2014.

Raymond T. Ng and Jiawei Han. Clarans: A method for clustering objects for spatial data mining. *IEEE transactions on knowledge and data engineering*, 14(5):1003–1016, 2002.

Andrei V Novikov. Pyclustering: Data mining library. *Journal of Open Source Software*, 4(36):1230, 2019.

Adeiza James Onumanyi, Daisy Nkele Molokomme, Sherrin John Isaac, and Adnan M. Abu-Mahfouz. Autoelbow: An automatic elbow detection method for estimating the number of clusters in a dataset. *Applied Sciences*, 12(15), 2022. ISSN 2076-3417. doi: 10.3390/app12157515. URL https://www.mdpi.com/2076-3417/12/15/7515.

Umut Orhan, Mahmut Hekim, and Mahmut Ozer. Eeg signals classification using the k-means clustering and a multilayer perceptron neural network model. *Expert Systems with Applications*, 38(10):13475–13481, 2011.

Bidyut Kr Patra, Sukumar Nandi, and P Viswanath. A distance based clustering method for arbitrary shaped clusters in large datasets. *Pattern Recognition*, 44(12):2862–2870, 2011.

F. Pedregosa, G. Varoquaux, A. Gramfort, V. Michel, B. Thirion, O. Grisel, M. Blondel, P. Prettenhofer, R. Weiss, V. Dubourg, J. Vanderplas, A. Passos, D. Cournapeau, M. Brucher, M. Perrot, and E. Duchesnay. Scikit-learn: Machine learning in Python. *Journal of Machine Learning Research*, 12:2825–2830, 2011.

Eduardo Machado Real, Maria Do Carmo Nicoletti, and Osvaldo Luiz De Oliveira. A closer look into sequential clustering algorithms and associated post-processing refinement strategies. *Int. J. Innov. Comput. Appl.*, 6(1):1–12, August 2014. ISSN 1751-648X. doi: 10.1504/IJICA.2014.064214. URL https://doi.org/10.1504/IJICA.2014.064214.

Peter J Rousseeuw. Silhouettes: a graphical aid to the interpretation and validation of cluster analysis. *Journal of computational and applied mathematics*, 20:53–65, 1987.

Michael C Rush and Joyce EA Russell. Leader prototypes and prototype-contingent consensus in leader behavior descriptions. *Journal of Experimental Social Psychology*, 24(1):88–104, 1988.

Alexander Schick, Mika Fischer, and Rainer Stiefelhagen. Measuring and evaluating the compactness of superpixels. In *Proceedings of the 21st international conference on pattern recognition (ICPR2012)*, pp. 930–934. IEEE, 2012.

Erich Schubert, Jörg Sander, Martin Ester, Hans Peter Kriegel, and Xiaowei Xu. Dbscan revisited, revisited: why and how you should (still) use dbscan. *ACM Transactions on Database Systems (TODS)*, 42(3):1–21, 2017.

M Steinbach and G Karypis. V. kumar,"a comparison of document clustering techniques". In *Proceeding of Text Mining Workshop, KDD*, 2000.

David Stutz, Alexander Hermans, and Bastian Leibe. Superpixels: An evaluation of the state-of-the-art. *Computer Vision and Image Understanding*, 166:1–27, 2018.

Sergios Theodoridis and Konstantinos Koutroumbas. *Pattern Recognition*. Elsevier Science Limited, 2006.

Robert Tibshirani, Guenther Walther, and Trevor Hastie. Estimating the number of clusters in a data set via the gap statistic. *Journal of the Royal Statistical Society: Series B (Statistical Methodology)*, 63(2):411–423, 2001. doi: https://doi.org/10.1111/1467-9868.00293. URL https://rss.onlinelibrary.wiley.com/doi/abs/10.1111/1467-9868.00293.

Kushal Tirumala, Daniel Simig, Armen Aghajanyan, and Ari Morcos. D4: Improving llm pretraining via document de-duplication and diversification. *Advances in Neural Information Processing Systems*, 36:53983–53995, 2023.

Lyle H Ungar and Dean P Foster. Clustering methods for collaborative filtering. In *AAAI workshop on recommendation systems*, volume 1, pp. 114–129. Menlo Park, CA, 1998.

Michael Van den Bergh, Xavier Boix, Gemma Roig, and Luc Van Gool. Seeds: Superpixels extracted via energy-driven sampling. *International Journal of Computer Vision*, 111:298–314, 2015.

Stéfan van der Walt, Johannes L. Schönberger, Juan Nunez-Iglesias, François Boulogne, Joshua D. Warner, Neil Yager, Emmanuelle Gouillart, Tony Yu, and the scikit-image contributors. scikit-image: image processing in Python. *PeerJ*, 2:e453, 6 2014. ISSN 2167-8359. doi: 10.7717/peerj.453. URL https://doi.org/10.7717/peerj.453.

David C Van Essen, Stephen M Smith, Deanna M Barch, Timothy EJ Behrens, Essa Yacoub, Kamil Ugurbil, Wu-Minn HCP Consortium, et al. The wu-minn human connectome project: an overview. *Neuroimage*, 80:62–79, 2013.

Andrea Vedaldi and Stefano Soatto. Quick shift and kernel methods for mode seeking. In *Computer Vision–ECCV 2008: 10th European Conference on Computer Vision, Marseille, France, October 12-18, 2008, Proceedings, Part IV 10*, pp. 705–718. Springer, 2008.

Ulrike Von Luxburg. A tutorial on spectral clustering. *Statistics and computing*, 17:395–416, 2007.

Patrick Wagner, Nils Strodthoff, Ralf-Dieter Bousseljot, Dieter Kreiseler, Fatima Lunze, Wojciech Samek, and Tobias Schaeffter. Ptb-xl, a large publicly available electrocardiography dataset. *Scientific Data*, 7:154, 2020. doi: 10.1038/s41597-020-0495-6. URL https://doi.org/10.1038/s41597-020-0495-6.

Rui Xu and Donald C Wunsch. Clustering algorithms in biomedical research: a review. *IEEE reviews in biomedical engineering*, 3:120–154, 2010.

Tian Zhang, Raghu Ramakrishnan, and Miron Livny. Birch: an efficient data clustering method for very large databases. *ACM sigmod record*, 25(2):103–114, 1996.

Ying Zhao and George Karypis. Data clustering in life sciences. *Molecular biotechnology*, 31:55–80, 2005.

A APPENDIX

A.1 APPARENT CENTROID METRIC

In this work Apparent Centroid distance (AC) was introduced which is a strict criterion to evaluate clustering results using the predicted centroids.

The metric is calculated as follows. The complete distance matrix between all estimated and ground truth centroids is created. We count the number of centroids that are close to the ground truth lesser than a pre-specified thresholds. AC is bounded between 0 and 1. The recommended threshold is at 10% of the circumscribed radius of size θ. This is why we use 0.1 for all relevant experiments. We have found that AC will drop quickly when even a small number of incorrect centroids are found. Which is not the case with other metrics reported. This allows a quantifiable identification of issues that are rather easy for humans. See Fig. A6-A17 and table 1.

A.2 HYPER-PARAMETER SELECTION AND SENSITIVITY

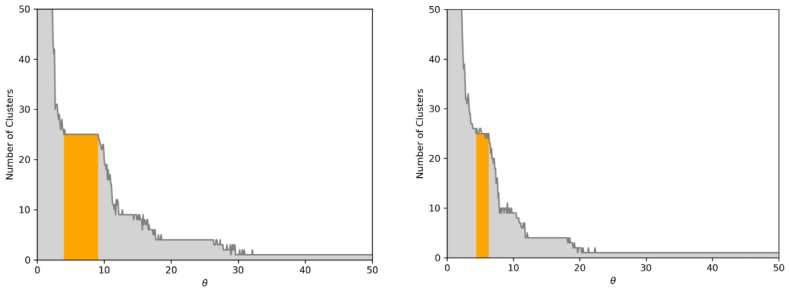

Figure A1: θ is often easier to find than K. Correct number of clusters and corresponding θ ranges were identified in the highlighted regions.

In this experiment, we add two dimensional normal distributions of identity covariance matrix in a grid of either axes of dimensions -22 to 22 separated in 5 equal spaces (see Fig. A1-Left) or -15 to 15 at 5 equidistant spaces (see Fig. A1-Right). The left has clusters with more space in-between them and the right less, i.e. clusters are closer. We sample 100 points from each distribution in each grid position. Note that true number of clusters which is actually 25 in both cases is easily found by just looking for plateaus in the graphs shown in Fig. A1. Therefore, θ can be robust in areas capturing the correct number of clusters (see highlight). In summary, there are only 4-5 plateus in this diagrams. The alternative would be to search K one by one. Such plots can be even easier to use if we also include the sum of intra class differences, then we can separate between the plateaus. For example, the highlighted regions minimize at the same time the sum of intraclass distances (also known as WCSS, within-cluster sum of squares).

A.3 LARGE SIMULATION EXPERIMENT - PARAMETERS

The following parameters were used for each method of the large comparisons experiment. Gaussian Mixture Models (tied covariance, maxiter=200, 5 initializations) (Moon, 1996), TB/TS/TSR/TBSCAN (θ 3.6, R 10, eps 2, min_samples 1), Bisecting KMeans (1 initialization, K 300), DBSCAN (eps 0.5 and min_samples 40), HDBSCAN (min_samples 40), KMeans++ (I 1, K 300), MeanShift (bandwidth 2.6), TBK (θ 3.6, K 300), FCM (n_clusters 300, expon 2, error 0.005, maxiter 1000) (Bezdek et al., 1984), MeanShift++ (bandwidth 3.4, threshold 0.00001, iterations 1000), OPTICS (min_samples 40, xi=0.05, min_cluster_size=5) (Ankerst et al., 1999), BSAS(theta 3.6, K 300), MBSAS (theta 3.6, K 300), TTSAS (threshold1 3.6, threshold2 4), BIRCH (threshold 2.5, branching_factor 500, n_clusters=K), CURE(n_clusters K, rep_points 1, compression 1) (Guha et al., 1998), KMEDIANS (K 300) (Moshkovitz et al., 2020b), CLARANS (K 300, numlocal 6, maxneighbor 4) (Ng & Han, 2002). KMEDOIDS (Moshkovitz et al., 2020a), AFFINITY PROPAGATION (Dueck, 2009), SPECTRAL (Von Luxburg, 2007) and HIERARCHICAL CLUSTERING cannot run due to extensive memory requirements (> 100 GBytes of RAM).

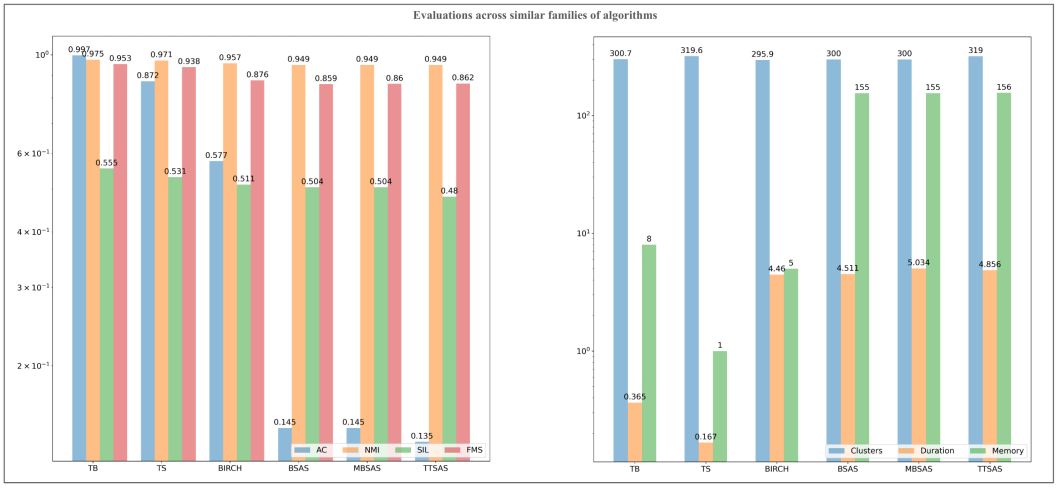

Figure A2: Summary plots with notable observations. Reporting AC, NMI, SIL, FMS, #clusters, runtime (duration in seconds), and peak memory (MBytes). Comparisons between families of algorithms that are distance-based and have common ground with TB. Note that TB has the highest scores while having the second fastest runtime after TS. For a complete list of comparisons see Table 1.

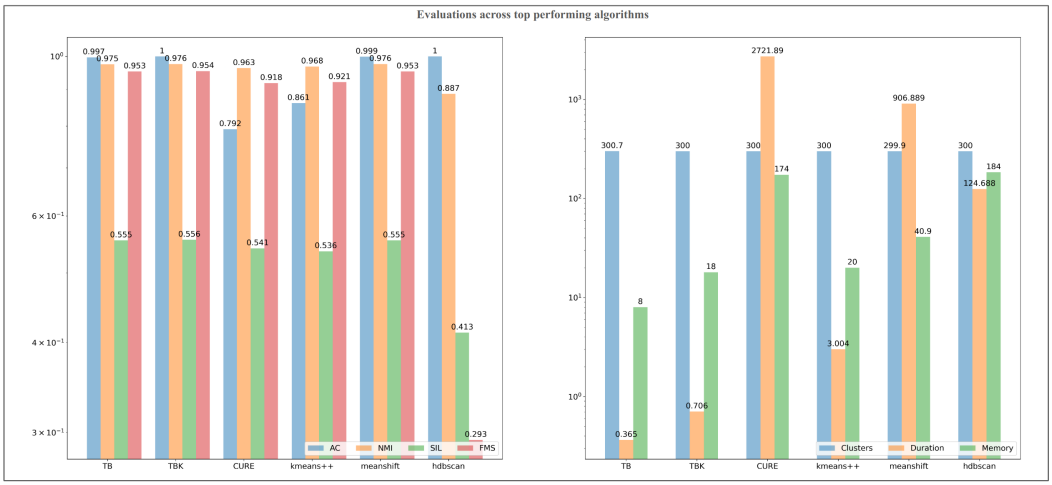

Figure A3: Comparisons between the 6 top performing algorithms in regards to AC. Note that TB matches the performance of algorithms while being 2484X faster and using 5X less memory than MeanShift and 342X faster and using 23X less memory than HDBSCAN. For a complete list of comparisons see Table 1.

A.4 Large Simulation Experiment - Visuals

In support of the large comparisons experiment of section 5.1 we present results of a range of algorithms. Different colors encode different clusters. Blue crosses ground truth centroids and red crosses encode estimated centroids.

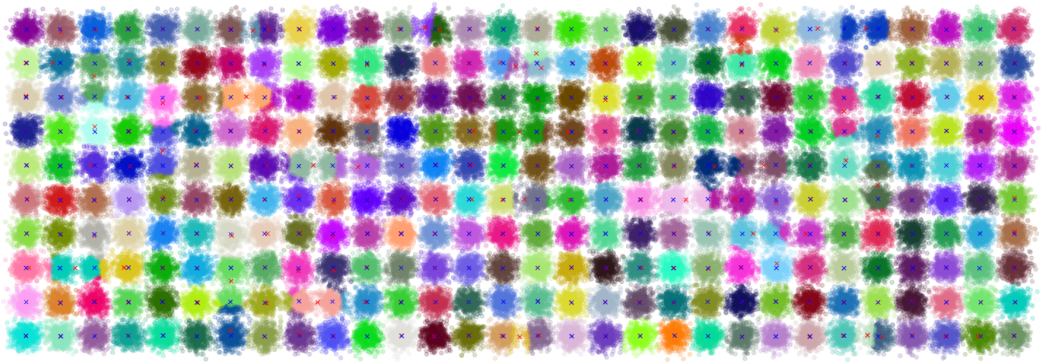

Figure A4: BIRCH ($threshold 2.5, branching\_factor 500, n\_clusters = 300$)

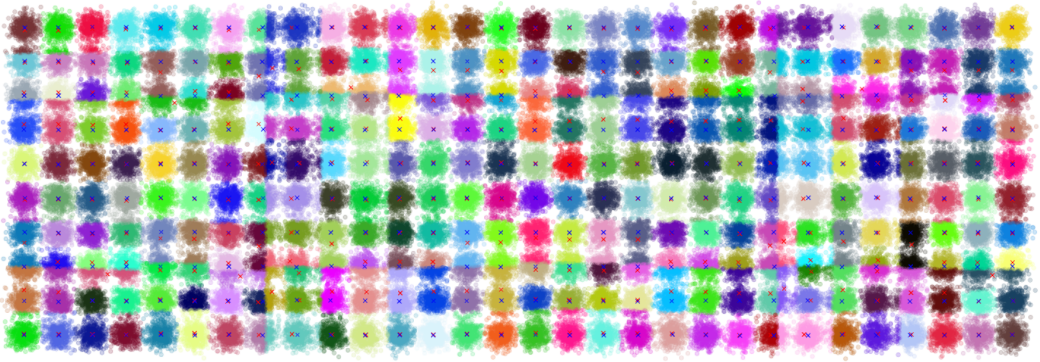

Figure A5: Bisecting KMeans ($1 initialization, K = 300$)

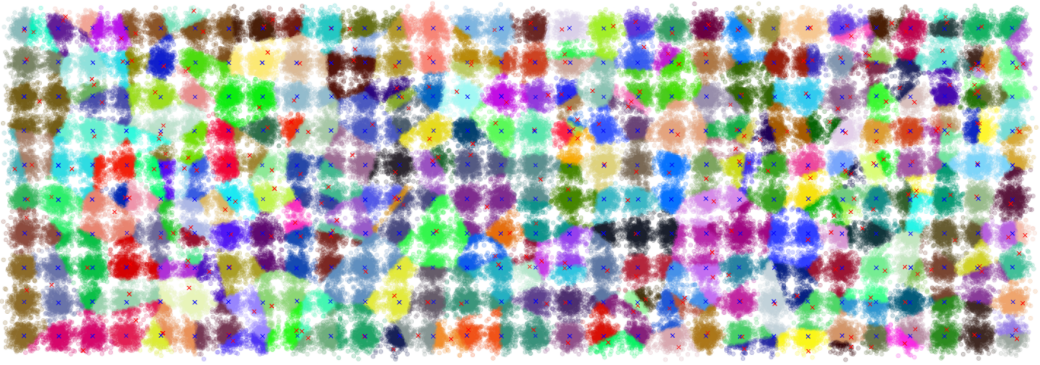

Figure A6: CLARANS ($K = 300, numlocal = 6, maxneighbor = 4$)

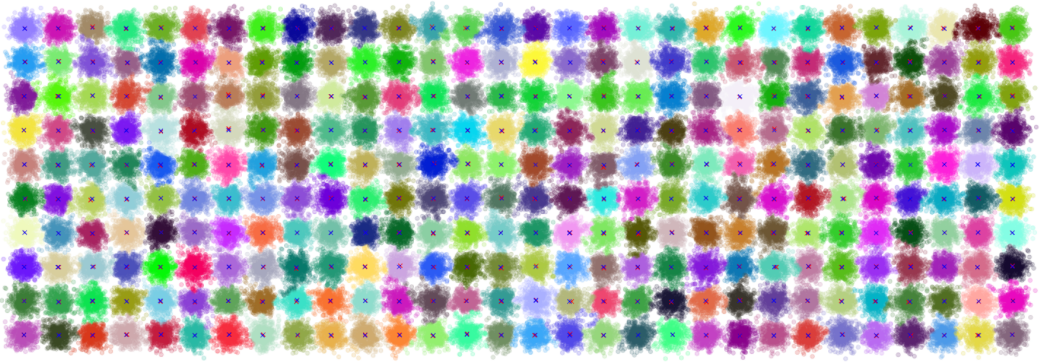

Figure A7: CURE ($n\_clusters = 300, rep\_points = 1, compression = 1$)

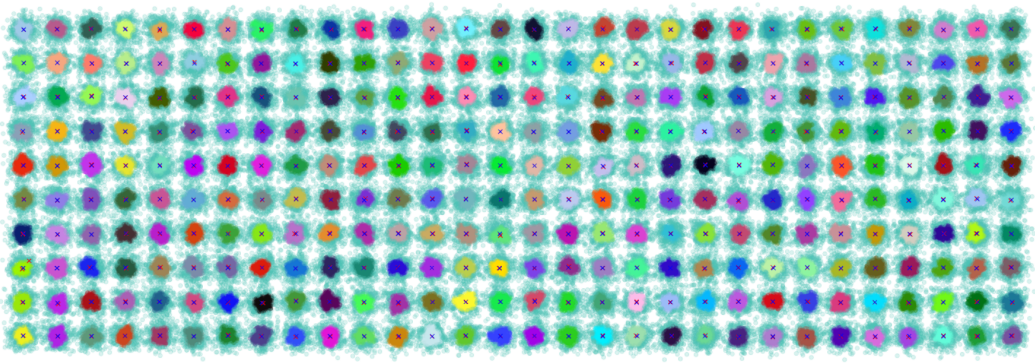

Figure A8: DBSCAN ($eps = 0.5, min\_samples = 40$)

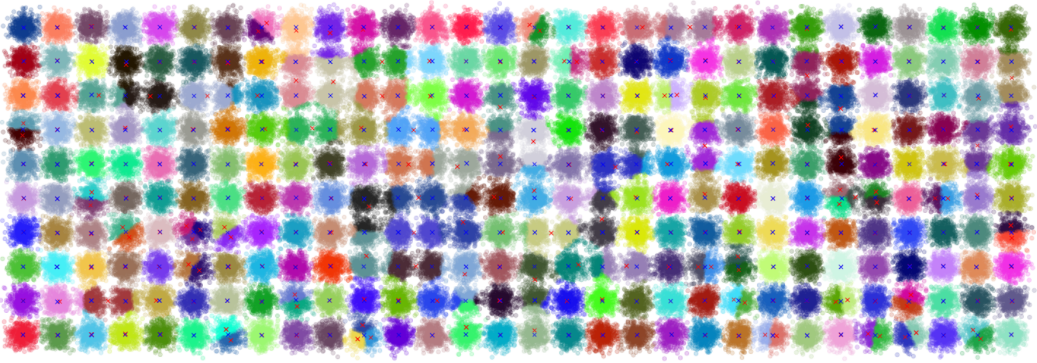

Figure A9: KMeans ($K = 300$)

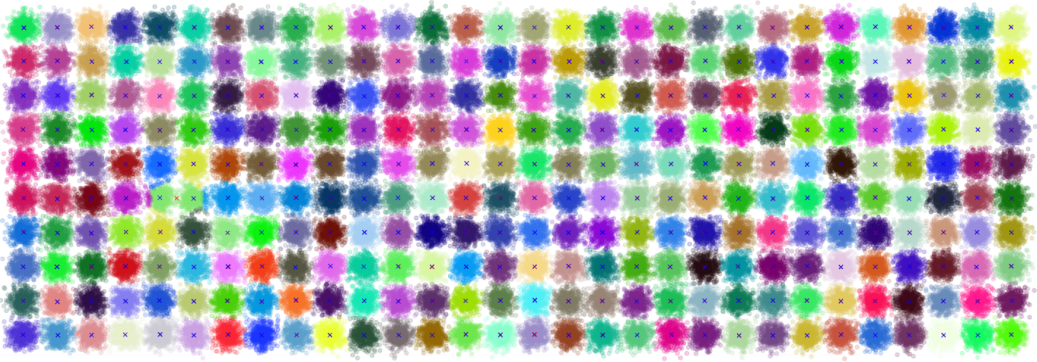

Figure A10: MeanShift ($bandwidth 2.6$)

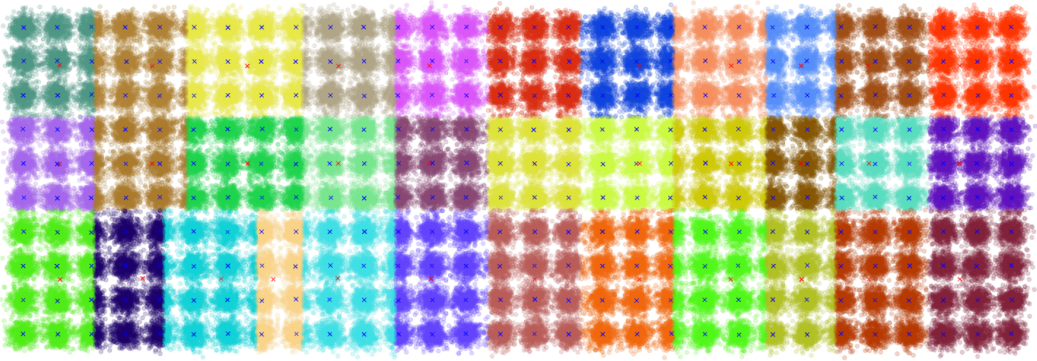

Figure A11: MeanShift++ ($bandwidth = 3.4, threshold = 0.00001, iterations = 1000$)

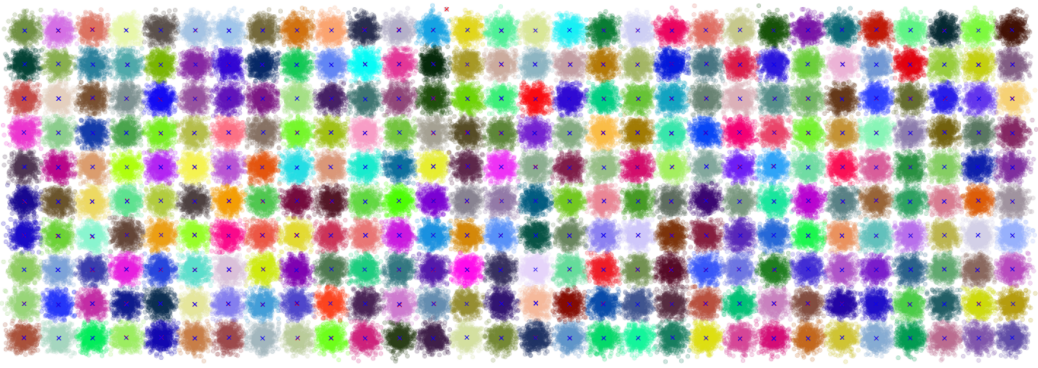

Figure A12: TB (θ=3.6)

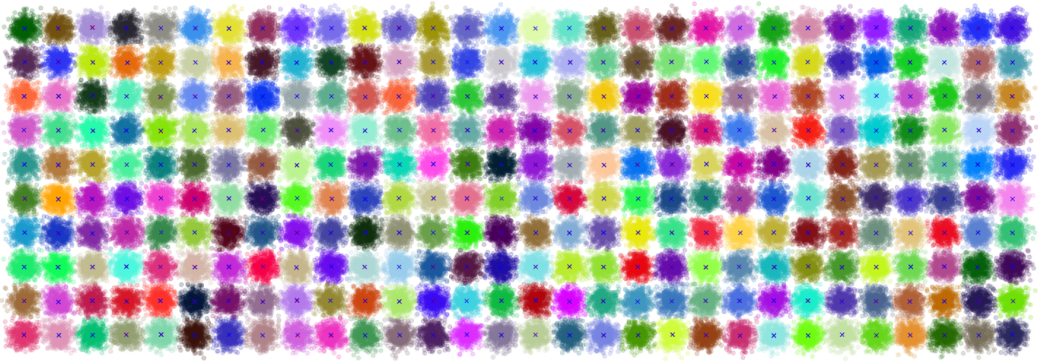

Figure A13: TBK (θ=3.6)

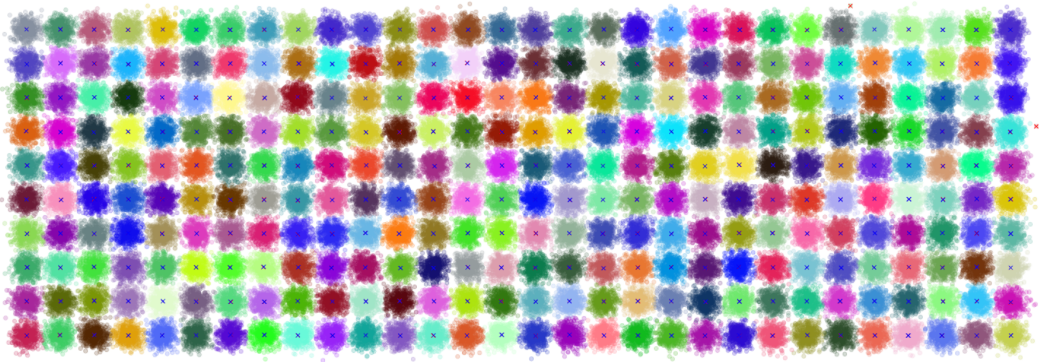

Figure A14: TBSCAN (θ=3.6, R=10, eps=2, min_samples=1)

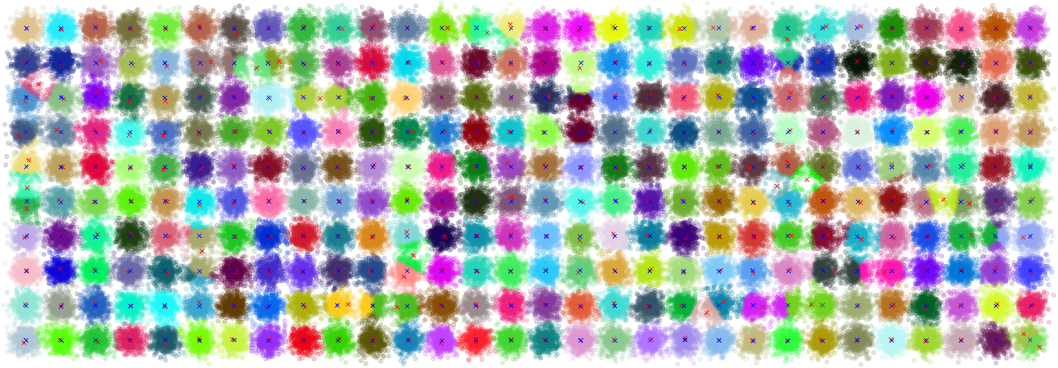

Figure A15: BSAS ($theta = 3.6, K = 300$)

A.5 SIGNAL PROCESSING OF TIME SERIES

Here, we demonstrate the use of TB to identify patterns in one-dimensional signals that change over time. For this purpose, we use common signals such as sine, pulse or combined sine and pulse signals. We also use the publicly available PTB-XL Electrocardiography (ECG) dataset (Wagner et al., 2020). From Fig. A16 to A26, we show the results obtained using TB. For Figs. A16 to A18, we use a small sliding window of 3, 5 and 3 respectively. This sliding window becomes our feature space. We then normalize the signal by scaling the data. Therefore, we move from a 1D signal to a 2D array $\boldsymbol{X}$ where the number of rows is as many as the samples of the signal and the number of columns is the size of the sliding window. TB is then applied to this 2D array with θ values of 90, 130 and 95 respectively.
For ECG Signals, we performed two types of pre-processing. In the first type of pre-processing, we used a Gaussian filter with $\sigma = 9$ for Fig. A19, $\sigma = 6$ for Fig. A20 and $\sigma = 11$ for Fig. A21. We then used a sliding window of size of 3, 7 and 3 respectively. In the second type of pre-processing, i.e, for Fig. A22 and Fig. A26, we used the entire dataset along with time as the feature space. Sliding windows and Gaussian filter were not used in this method. The θ values that were used are 1, 6, 26, 90 and 50 respectively. We then normalize the signal in both the cases by scaling the data. As shown in Fig. A16 to A26, TB with L^2 is able to identify the patterns in the signal without needing to calculate the derivatives (Duan & Guo, 2022). In the case of the PTB-XL ECG dataset, TB is able to identify the QRS and T-wave together (Fig. A19), or as QR, RS and T-wave separately (Fig. A20) or as QRS and T-wave separately (Fig. A21) (Maglaveras et al., 1998). We can also capture the full cardiac cycles as discrete groups as shown in Fig. A22 and Fig. A26.

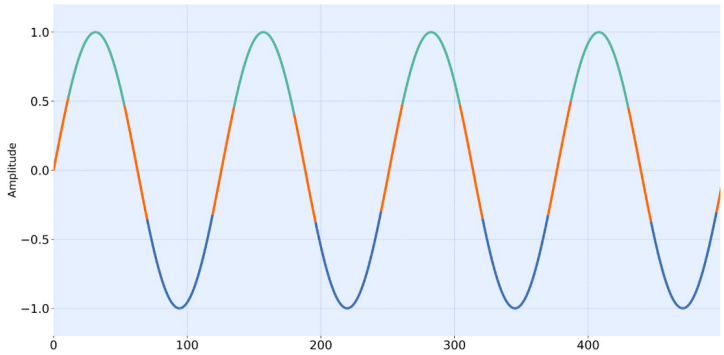

Figure A16: Patterns in Sine wave identified with TB.

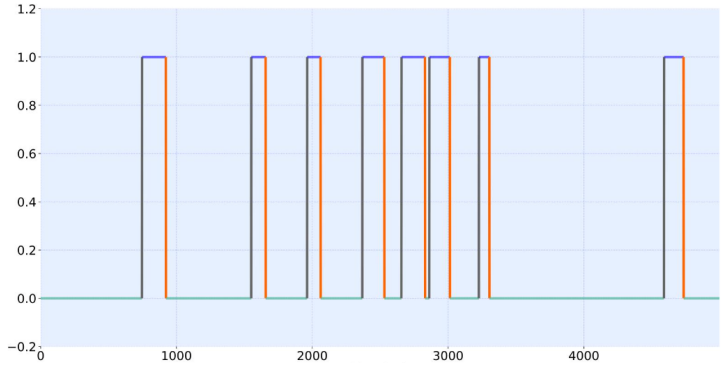

Figure A17: Patterns in Pulse signals identified with TB

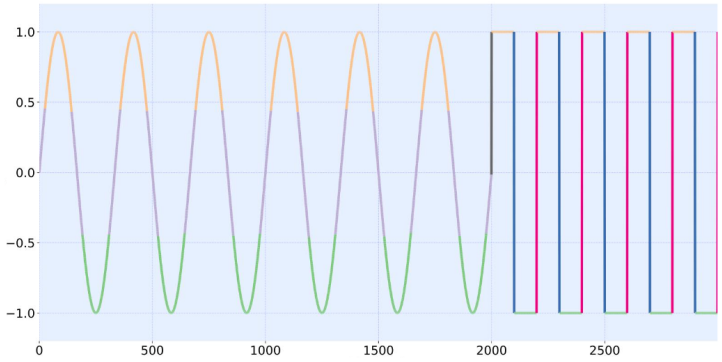

Figure A18: Patterns in Combined signal identified with TB (example 1)

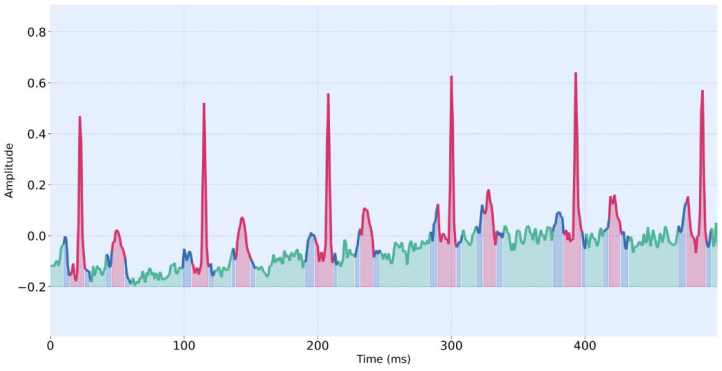

Figure A19: Patterns in ECG signals identified with TB (example 1)

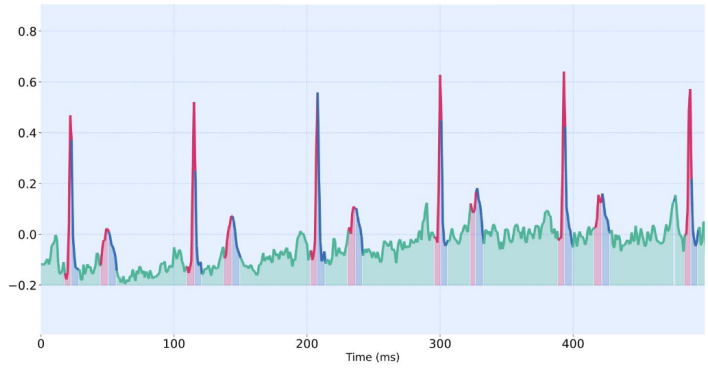

Figure A20: Patterns in ECG signals identified with TB (example 2)

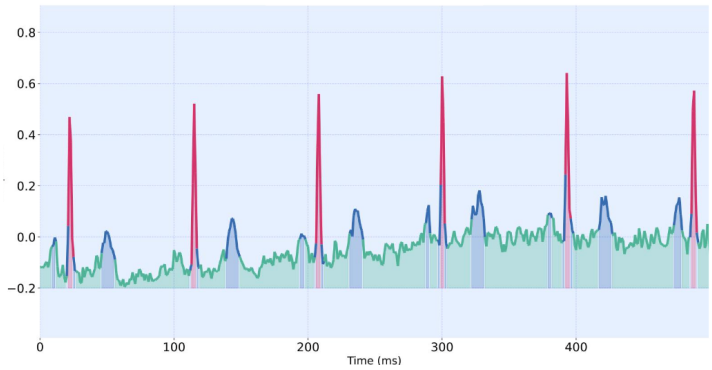

Figure A21: Patterns in ECG signals identified with TB (example 3)

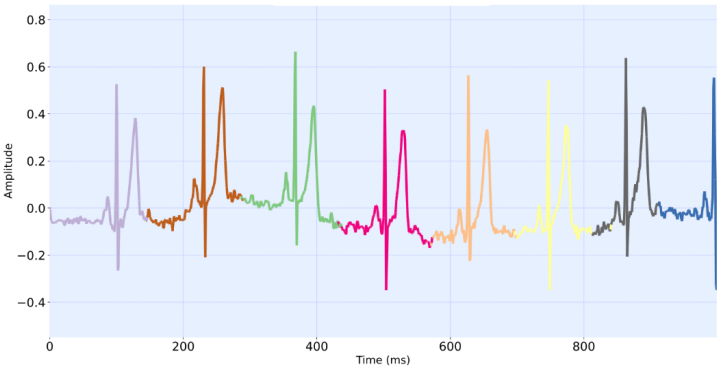

Figure A22: Patterns in ECG signals identified with TB (example 4)

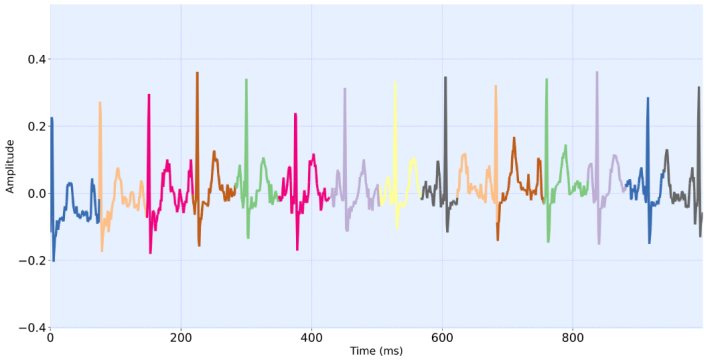

Figure A23: Patterns in ECG signals identified with TB (example 5)

A.6 Additional information on benchmarks

The parameters used for the linearly and non-linearly separable datasets shown in section 5.2 are summarized in the tables below.

The table A1 demonstrates exceptional performance across all metrics (NCA, RI, FM, ARI, NMI) by TB method, achieving nearly perfect clustering results with remarkably low runtime compared to K-means, Birch, and Meanshift. TB consistently outperforms the other algorithms in efficiency, making it ideal for real-time or resource-constrained scenarios. However, TB may not inherently support non-linear separability, which could limit its application to datasets with more complex structures. TBSCAN has been introduced for this exact reason. As we can observe on table A2, TBSCAN stands out by maintaining excellent clustering performance (NCA, RI, FM, ARI, NMI), rivaling HDBSCAN and Agglomerative Clustering (single linkage), but with significantly lower runtime. A small note that other linkage type (ward, complete, average) has been tested with Agglomerative Clustering. However, we could not achieve excellent clustering so they had to be disclosed for a fair comparison.

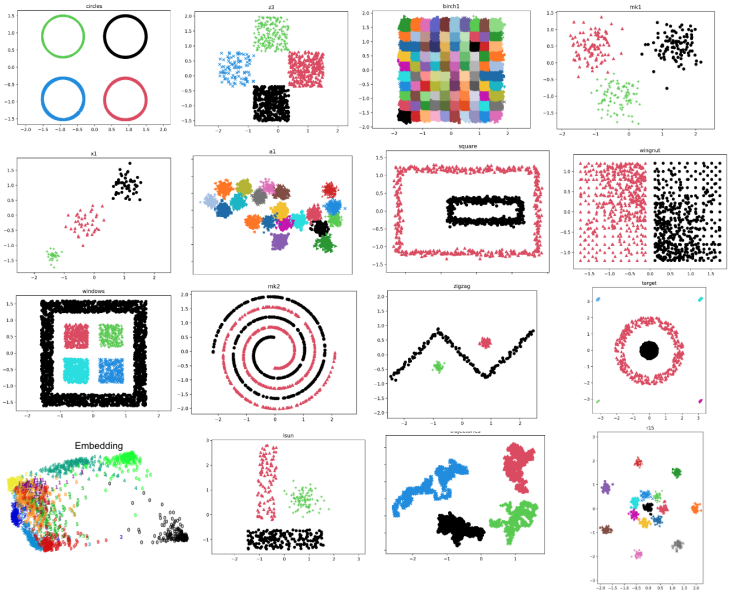

Linear and Non-Linear datasets used for the benchmark experiments

Table A1: Performance Comparisons of Linear benchmarks.

TB on Linearly Separable Datasets							
Dataset	Clusters	Runtime ↓	NCA ↑	RI ↑	FM ↑	ARI ↑	NMI ↑
circles	4/4	**0.00091**	1.0	1.0	1.0	1.0	1.0
z3	4/4	**0.00053**	1.0	1.0	1.0	1.0	1.0
birch1	101/100	**0.07872**	0.97	0.99	0.97	0.96	0.98
mk1	3/3	**0.00017**	0.99	0.99	0.99	0.98	0.98
trajectories	4/4	**0.00219**	0.99	0.99	0.99	0.99	0.99
x1	3/3	**0.00013**	1.0	1.0	1.0	1.0	1.0
a1	24/20	**0.00091**	0.81	0.99	0.99	0.95	0.96
r15	8/8	**0.00031**	1.0	1.0	1.0	1.0	1.0
K-means on Linearly Separable Datasets							
Dataset	Clusters	Runtime ↓	NCA ↑	RI ↑	FM ↑	ARI ↑	NMI ↑
circles	4/4	0.00634179	1.0	1.0	1.0	1.0	1.0
z3	4/4	0.00363559	1.0	1.0	1.0	1.0	1.0
birch1	100/100	0.53998762	0.95681	0.99888	0.96278	0.94378	0.97568
mk1	3/3	0.00116613	0.99502	0.99556	0.99668	0.98998	0.98299
trajectories	4/4	0.01502252	0.99987	0.99990	0.99993	0.99973	0.99936
x1	3/3	0.00089175	1.0	1.0	1.0	1.0	1.0
a1	25/20	0.00624223	0.98282	0.99682	0.99833	0.96634	0.97381
r15	8/8	0.00212648	1.0	1.0	1.0	1.0	1.0
Birch on Linearly Separable Datasets							
Dataset	Clusters	Runtime ↓	NCA ↑	RI ↑	FM ↑	ARI ↑	NMI ↑
circles	4/4	0.01960280	1.0	1.0	1.0	1.0	1.0
z3	4/4	0.01141702	1.0	1.0	1.0	1.0	1.0
birch1	100/100	1.69575003	0.89768	0.91556	0.9602470	0.95321	0.966945
mk1	3/3	0.00366206	0.99502	0.99556	0.99668	0.98998	0.98299
trajectories	4/4	0.04717597	1.0	1.0	1.0	1.0	1.0
x1	3/3	0.0028004	1.0	1.0	1.0	1.0	1.0
a1	23/20	0.0196028	0.79705	0.99222	0.99591	0.91804	0.95122
r15	8/8	0.00667788	1.0	1.0	1.0	1.0	1.0
Meanshift on Linearly Separable Datasets							
Dataset	Clusters	Runtime ↓	NCA ↑	RI ↑	FM ↑	ARI ↑	NMI ↑
circles	4/4	2.64446	1.0	1.0	1.0	1.0	1.0
z3	4/4	1.54018	1.0	1.0	1.0	1.0	1.0
birch1	101/100	228.76032	0.96543	0.981043	0.960004	0.957838	0.9785959
mk1	3/3	0.49402	0.99	0.99	0.99	0.98	0.98
trajectories	4/4	6.36414	0.99	0.99	0.99	0.99	0.99
x1	3/3	0.37778	1.0	1.0	1.0	1.0	1.0
a1	25/20	2.64446	0.86	0.98	0.97	0.96	0.97
r15	8/8	0.90086	1.0	1.0	1.0	1.0	1.0

Table A2: Performance Comparisons of Non-Linear benchmarks.

TBSCAN on Non-Linearly Separable Datasets							
Dataset	Clusters	Runtime ↓	NCA ↑	RI ↑	FM ↑	ARI ↑	NMI ↑
windows	5/5	**0.007092875**	1.0	1.0	1.0	1.0	1.0
square	2/2	**0.001162792**	1.0	1.0	1.0	1.0	1.0
wingnut	2/2	**0.001298250**	1.0	1.0	1.0	1.0	1.0
zigzag	3/3	**0.000820125**	1.0	1.0	1.0	1.0	1.0
target	6/6	**0.002047375**	1.0	1.0	1.0	1.0	1.0
lsun	3/3	**0.001416042**	1.0	1.0	1.0	1.0	1.0
mk2	2/2	**0.003112458**	1.0	1.0	1.0	1.0	1.0
HDBSCAN on Non-Linearly Separable Datasets							
Dataset	Clusters	Runtime ↓	NCA ↑	RI ↑	FM ↑	ARI ↑	NMI ↑
windows	5/5	0.038237875	1.0	1.0	1.0	1.0	1.0
square	2/2	0.016157084	1.0	1.0	1.0	1.0	1.0
wingnut	2/2	0.019175417	1.0	1.0	1.0	1.0	1.0
zigzag	3/3	0.002936958	1.0	1.0	1.0	1.0	1.0
target	3/6	0.006192208	0.50000	0.99982	0.99982	0.99963	0.98602
lsun	3/3	0.004924541	1.0	1.0	1.0	1.0	1.0
mk2	2/2	0.017242167	1.0	1.0	1.0	1.0	1.0
Agglomerative Clustering (Single Linkage) on Non-Linearly Separable Datasets							
Dataset	Clusters	Runtime ↓	NCA ↑	RI ↑	FM ↑	ARI ↑	NMI ↑
windows	5/5	0.029719333	1.0	1.0	1.0	1.0	1.0
square	2/2	0.005899709	1.0	1.0	1.0	1.0	1.0
wingnut	2/2	0.006111000	1.0	1.0	1.0	1.0	1.0
zigzag	3/3	0.001121333	1.0	1.0	1.0	1.0	1.0
target	6/6	0.004177458	1.0	1.0	1.0	1.0	1.0
lsun	3/3	0.002066667	1.0	1.0	1.0	1.0	1.0
mk2	2/2	0.005654750	1.0	1.0	1.0	1.0	1.0
Spectral Clustering on Non-Linearly Separable Datasets							
Dataset	Clusters	Runtime ↓	NCA ↑	RI ↑	FM ↑	ARI ↑	NMI ↑
windows	5/5	3.573450375	0.76499	0.56371	0.68490	0.08047	0.36880
square	2/2	0.568301875	0.61350	0.56802	0.47644	0.13638	0.25496
wingnut	2/2	0.374673375	0.86220	0.87157	0.87170	0.74314	0.63820
zigzag	3/3	0.023156958	0.47152	0.70699	0.80126	0.30452	0.46853
target	6/6	0.502081875	0.28023	0.69488	0.67860	0.39250	0.48070
lsun	3/3	0.296371333	0.87513	0.89550	0.91390	0.78268	0.80938
mk2	2/2	0.460497625	0.08236	0.50286	0.50228	0.00573	0.00488

Table A3: Performance Comparisons on Digits dataset vs HC.

Methods	Clusters	Runtime ↓	Peak Memory ↓	NCA ↑	RI ↑	FM ↑	ARI ↑	NMI ↑
HC-Ward	10/10	0.028286958	13.8585	**0.5896**	**0.9049**	**0.9467**	**0.5129**	**0.6291**
HC-Average	10/10	0.027868458	13.8541	0.5383	0.8526	0.9151	0.4179	0.6139
HC-Complete	10/10	0.025582417	13.8534	0.4858	0.8589	0.9194	0.3844	0.5702
HC-Single	10/10	0.014241500	0.2104	0.1960	0.2801	0.4478	0.0447	0.2418
TB	10/10	**0.000827417**	**0.1469**	0.5222	0.8425	0.9092	0.3749	0.5752

Table A4: TB/TBSCAN Parameters for Linearly/Non-Linearly Separable Datasets experiments

Linear Dataset	θ	Non-Linear Dataset	θ	Min Samples	EPS
circles	1.2	trajectories	0.1	1	0.3
z3	1.1	windows	0.1	1	0.3
birch1	0.25	square	0.2	1	0.4
mk1	1.5	wingnut	0.25	1	0.42
unbalance	0.35	zigzag	0.25	1	0.5
x1	1	target	0.1	1	0.5
a1	0.3	lsun	0.1	1	0.35
r15	1	mk2	0.05	1	0.35

A.7 ADDITIONAL SUPERPIXEL EXPERIMENTS

We present two results as additional information on superpixel application. Fig. A24 compares TB against K-means++, Meanshift and Meanshift++ for creating superpixel segments. Superpixel labels and the averaged images are shown using two examples from the BSD500 (first and second row) and NYUV2 dataset (third and fourth row).

Fig. A25 presents how the change in number of superpixels (or clusters) affect the metrics on TB, compared to SLIC with different parameters and Meanshift, Meanshift++. The metrics were evaluated on the BSD500 dataset. Since the dataset contains multiple labels per image, the metrics were first calculated for all labels of the image and averaged. The value on the plot shows an average of such values from 500 images of the dataset.

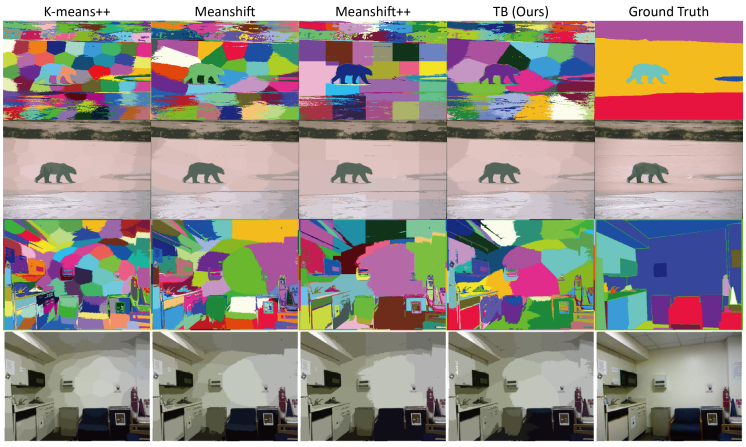

Figure A24: Superpixel comparison against other clustering methods

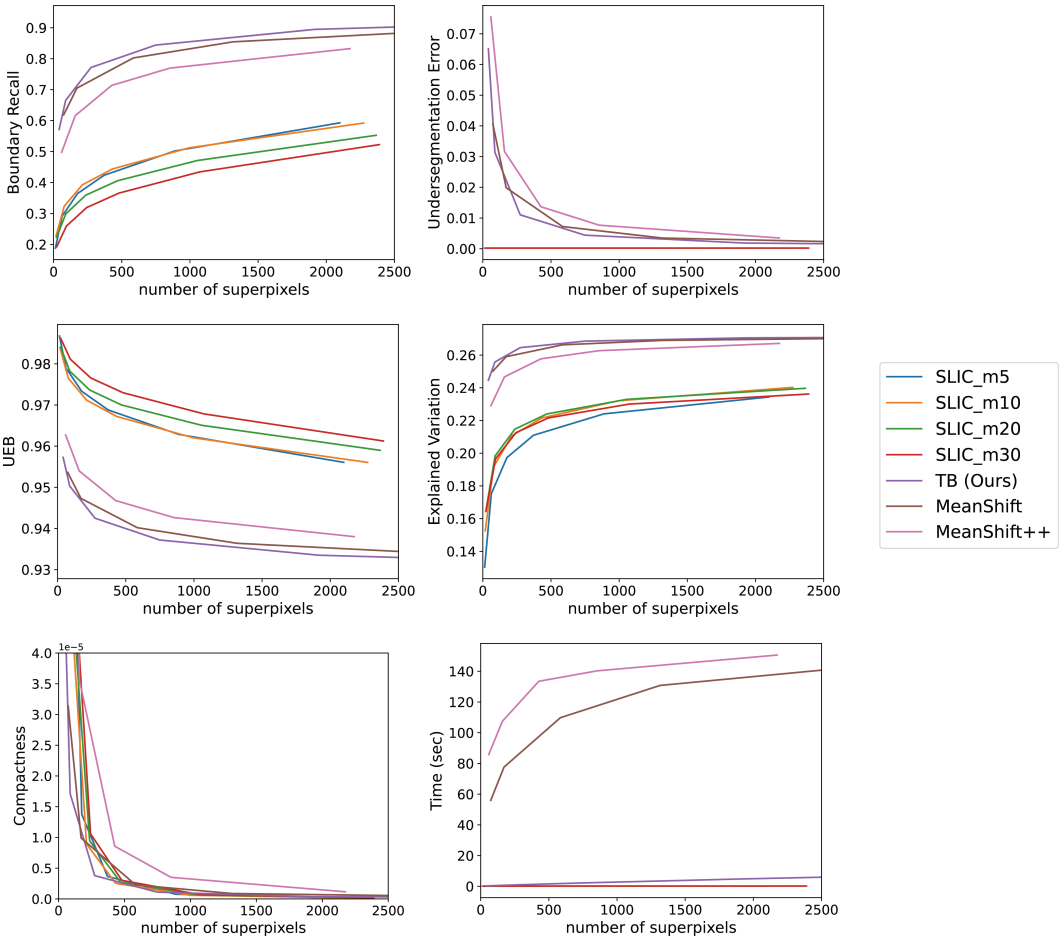

Figure A25: The plot shows how metrics are affected by the increase in number of superpixels.

A.8 PROVING RUNTIME

Theorem 4 The runtime complexity of Thetan Berseker (TB) in regards to distance calls is in the range of O (n) to O (n^2).

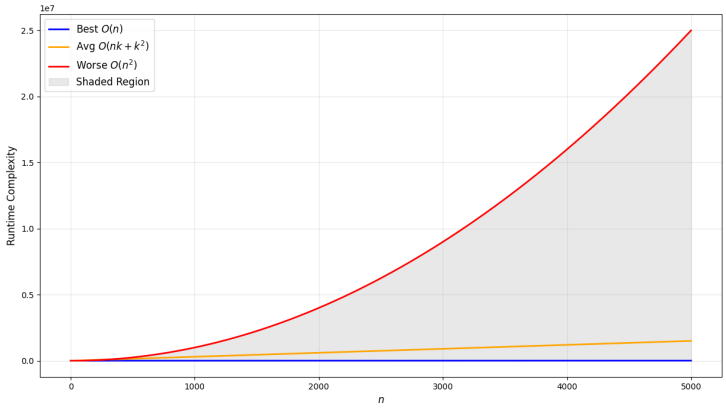

Figure A26: Thetan Berserker's runtime complexity is bounded between $\mathcal{O}(n)$ and $\mathcal{O}(n^2)$.

Proof Thetan Berserker (TB) consists of 4 steps as described in ablation study (see Fig. 3A). Two of the steps run Thetan Sequential (TS steps) and two run centroid updates and relabeling (CL steps).

We define N as the total number of samples and K the total number of clusters. In order to connect to the previous definitions we will use $T(N)/\mathrm{O}(N)$ rather than $T(n)/\mathrm{O}(n)$. In addition, we will omit D (feature space size) for now given that we look at complexity in regards to distance calls.

The worst Big-O time complexity for Thetan Sequencial is O (N^2). This is because most of compute time is spent on distance computations. Therefore in the case where each sample is a different cluster we obtain a total of $1 + 2 + 3 + ... + N - 1 = N(N-1)/2 = N^2/2 - N/2$ distances. This will run in length two times for TB.

The second time the centroids are pre-pended to the datasets of samples therefore now the total number of distance computations will be $1 + 2 + 3 + ... + N - 1$.

The CL steps of TB allow to merge centroids and update labels. The first part of CL involves running TS only on the M generated centroids. This will merge any centroids that have a neighbor centroid at distance closer than θ. The relabel step (RE) will update the final labels to account for the centroid updates. There are as many labels as the number of samples N. However, unique labels are only M. Putting all these together we can study the best, worse and average time complexity.

In worst case every sample is a singleton cluster and for this reason $K = N$. We can now separate the distance calls for each step of the algorithm.

Worst case $K = N$,

$$
\begin{aligned}
T(N) = & \left.\begin{array}{rl} & 1 + 2 + \cdots + (N-1)] \\ + & 1 + 2 + \cdots + (N-1)] \\ + & 0 \qquad\qquad\qquad\quad] \end{array}\right. \begin{array}{l} TS_1(X) \\ TS_1(M) \\ RE_1(N) \end{array} \Bigg] \; CL_1 \\
& \left.\begin{array}{rl} & + 1 + 2 + \cdots + (N-1) \\ + & N + N + \cdots + N \end{array}\right] \; TS_2(M + X) \\
& \left.\begin{array}{rl} & + 1 + 2 + \cdots + (N-1)] \\ + & 0 \qquad\qquad\qquad\quad] \end{array}\right. \begin{array}{l} TS_2(M) \\ RE_2(N) \end{array} \Bigg] \; CL_2
\end{aligned}
$$

Because there is nothing to relabel the number of distance calls is 0. Therefore $T(N) = 4N^2/2 - 4N/2 + N^2 = 3N^2 - 2N$ which means that worst case Big-O for runtime is O (N^2). The best case takes place when the data is represented by a single cluster. Best case $K = 1$,

$$
\begin{aligned}
T(N) = & \left.\begin{array}{rl} & 1 + 1 + \cdots + 1] \\ + & 1 + 1 + \cdots + 1] \\ + & 0 \qquad\qquad\quad] \end{array}\right. \begin{array}{l} TS_1(X) \\ TS_1(M) \\ RE_1(N) \end{array} \Bigg] \; CL_1 \\
& \left.\begin{array}{rl} & + 1 + 1 + \cdots + 1 \\ + & 1 + 1 + \cdots + 1 \end{array}\right] \; TS_2(M + X) \\
& \left.\begin{array}{rl} & + 1 + 1 + \cdots + 1] \\ + & 0 \qquad\qquad\quad] \end{array}\right. \begin{array}{l} TS_2(M) \\ RE_2(N) \end{array} \Bigg] \; CL_2
\end{aligned}
$$

Here, there is also no need for relabeling. As long as there are no new clusters being created. In other words $T(N) = 5N$, which means that the best case has complexity O (N).

We should also look at the average case. In most clustering problems the number of clusters are at least one order or many orders of magnitude less than the data samples. For example, for 1 million samples is not uncommon to search for 1 thousand clusters. Therefore, it is reasonable to assume that for an average case K is assumed to be smaller than N.

Average case, for $K << N$,

$$T(N) = \begin{array}{ll} 1+2+\cdots+(K-1)+(N-K-1)K] & TS_1(X) \\ +1+2+\cdots+(K-1) \quad] & TS_1(M) \\ +1+2+\cdots+(K-1) \quad] & RE_1(N) \\ +1+2+\cdots+(K-1)+NK \quad] & TS_2(M+X) \\ +1+2+\cdots+(K-1) \quad] & TS_2(M) \\ +1+2+\cdots+(K-1) \quad] & RE_2(N) \end{array} \begin{array}{l} \\ \\ \Big] CL_1 \\ \\ \\ \Big] CL_2 \end{array}$$

Which is equal to $T(N) = 2NK + 2.5K^2 - K - 3.5$. Therefore, average case is O $(NK + K^2)$. Given that K is much less than N the runtime will be closer to linear than quadratic. This completes the proof. ■

High dimensional data with large number of features D are expected to delay each distance computation in a constant matter. TB is used with $I = 2$ everywhere in this work. Given its fast convergence as shown in Fig. 3B we do not expect to see any surprises in regards to time complexity.

A.9 Proving memory

Lemma 3 The spatial complexity of Thetan Berserker is linear.

Proof The only memory generated is centroids and labels. Those are produced in a constant amount. Therefore, the spatial complexity is best case $T(N) = cN$, i.e. $\mathcal{O}(N)$ and worst case i.e. $T(N) = 2cN$, i.e. O (N). Where c is a constant. ■

A.10 Merging samples via Thetan Sequential

Clarifications on Algorithm 2. As Theorem 1 suggests TS works well when the clusters have inter-class distances greater than hyper-parameter θ. In other words, when there is plenty of empty spaces between the clusters. However, the first TS in TB generates centroids. These according to Theorem 2 are reduced representation of the original data. Due to TS being order sensitive it could be that some of the centroids might be closer than $theta$. Nonetheless, they will be sparser than the original data if a reasonable θ has been chosen. Therefore, the second TS that acts on the centroids (output of the first TS) will merge together any centroids that are closer than θ. See Fig. A27.

Proposition 1 The output centroids of TS of hyper-parameter θ will be merged by a second TS on the centroids, only if the centroids have in-between distances less than θ.

Proof Due to Theorem 1 any order of selection will lead to singleton clusters of points that are far from each other by a distance that is greater than θ. TS will generate such points but due to its order sensitivity may generate a few centroids that are also close to each other. Therefore, we have a scenario such as that of Fig. A27. In that case in order to prove this we need to look at all pairwise distances and order selections. For example, if TS processes points in this order 1, 2, 3, 4. The distances between 1 and 2 are greater than threshold (2 clusters), 2 and 3 less than threshold (2 and 3 gets merged) and 3, 4 greater than threshold (a new cluster). If we take any other ordering, for example 3, 1, 2, 4 we will conclude on the same result. Merging of 2 & 3. This is because the only small pairwise distance is between 2 and 3. This generalizes to any number of TS output centroids. ■

Overall, this is an efficient way to merge close points without calculating all pairwise distances.

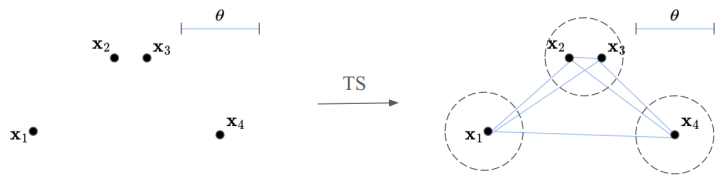

Figure A27: If distance θ has the size shown above any order of selection of the points will allow TS (Algorithm 1) to merge samples 2 and 3.

A.11 EFFICIENTLY UPDATING CENTROIDS

The centroids are updated on the fly using the following idea. The sum of samples for each cluster and the number of clusters are kept as different variables. To insert a new point x_i to a cluster we simply need to $\sum_k = \sum_k + x_i$ for each dimension D and then update $n_k = n_k + 1$. The centroid evaluation is then performed only when needed by dividing the sums by their corresponding n_ks.

A.12 FURTHER CLARIFICATIONS ON TB'S FAST CONVERGENCE

This section is expanding on the proof of Theorem 2. In Fig. A28 we see two square regions representing two uniform distributions that are close to each other by distance l. In the diagram l is set to be at $\theta/2$.

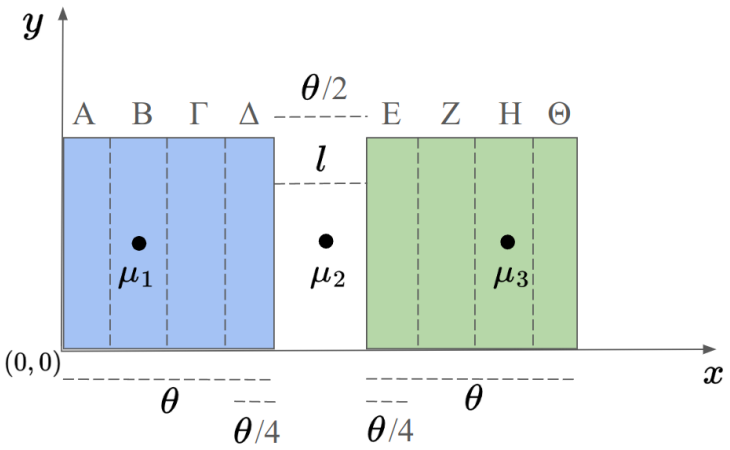

Figure A28: Two square uniform distributions (blue and green) of size size $\theta \times \theta$ containing an undetermined number of samples are at distance $l = \theta/2$. Greek letters separate the squares in equal bands.

Let $\boldsymbol{\mu}_1$, $\boldsymbol{\mu}_2$, and $\boldsymbol{\mu}_3$ represent undesired centroids obtained from the initial clustering process using TS (due to a bad order). Upon applying a further clustering process, i.e, TS $(\boldsymbol{M}, \boldsymbol{X})$ we encounter three possible cases:

Case 1: If the distance between $\boldsymbol{\mu}_1$ and $\boldsymbol{\mu}_2$ is less than the threshold θ, this results in two clusters:

- **Cluster 1** has a new centroid at position: $(\boldsymbol{\mu}_1 + \boldsymbol{\mu}_2)/2$
- **Cluster 2** has an updated centroid at position: $\boldsymbol{\mu}_3'$

Case 2: If the distance between $\boldsymbol{\mu}_2$, and $\boldsymbol{\mu}_3$ is less than θ, $\boldsymbol{\mu}_1$ is far from μ_2, this results in two clusters:

- **Cluster 1** has an updated centroid at position: $\boldsymbol{\mu}_1'$
- **Cluster 2** has a new centroid at position: $(\boldsymbol{\mu}_2 + \boldsymbol{\mu}_3)/2$

Case 3: If all in between distances are greater than θ then 3 clusters are obtained:

- **Cluster 1** has centroid at position: $\boldsymbol{\mu}_1$
- **Cluster 2** has centroid at position: $\boldsymbol{\mu}_2$
- **Cluster 3** has centroid at position: $\boldsymbol{\mu}_3$

Index here corresponds to the actual order. Meaning that $\boldsymbol{\mu}_1$ is the first point to be processed by TS$(\boldsymbol{M}, \boldsymbol{X})$. $\boldsymbol{\mu}_2$ is the second etc. It is important to note that these cases assume the distances between centroids are calculated using Euclidean distance.

The first two cases are highly desirable because the will help TB to have the two clusters separate and never provide 3 clusters. Therefore, case 1 and 2 clearly improve order sensitivity. Even if an upcoming point is at the edge of each distribution it will be pulled to the correct centroids and be assigned to the correct cluster.

The third case is problematic because it may continue supporting the idea that they may be three (incorrect) rather than two clusters (clusters). We can prove by contradiction that case 3 is highly unlikely. This also further explains why TB converges as fast as it does.

Proposition 1 Case 3 is not possible with the current setup.

Each uniform distribution (square) has θ sides. Let's assume that the origin of the coordinate system is at the bottom left corner of the blue square. Then $\boldsymbol{\mu}_2 = (\theta + \theta/4, \theta/2)$. Let's also assume that all three samples are at the same height (y value). Therefore we can reduce this to look only at the x axis.

As discussed in case 3 the distance between μ_1^x and μ_2^x is greater than θ. Therefore,

$$\begin{aligned} ||\mu_2^x - \mu_1^x|| &> \theta \\ \theta + \theta/4 - \mu_1^x &> \theta \\ \mu_1^x &< \theta/4 \end{aligned}$$

Also the distance between μ_2^x and μ_2^x is greater than θ, which means that

$$\begin{aligned} ||\mu_3^x - \mu_2^x|| &> \theta \\ \mu_3^x - \theta - \theta/4 &> \theta \\ \mu_3^x &> 2\theta + \theta/4 \end{aligned}$$

So if 3 centroids appear (rather than 2) two of them (μ_1^x and μ_3^x) will be forced to be at the bands A and Θ respectively. But if this is the case then μ_2^x will be representing bands $\mathrm{B}, \Gamma, \Delta, \mathrm{E}, \mathrm{Z}, \mathrm{H}$ and the empty space of width $\theta/2$. But this is a contradiction because the threshold is only θ not $7\theta/2$. In other words there is no ordering that can allow TS to generate centroids that will be at such distances apart. This completes the proof. ■

Here we showed this contradiction with two clusters but it is trivial to show the same for any number of uniform densities at $\theta/2$. The example shown here cannot cover all possible datasets but it gives a good idea for why the Berserker centroids help create more accurate upcoming centroids.

A.13 Using random walks for predicting the hyper-parameter

The approach in regards to Fig. 4A is elaborated in this section. A random walk in this case is accessing randomly samples from the available data matrix $\boldsymbol{X}$.

For example, one random walk will visit samples $\boldsymbol{x}_0, \boldsymbol{x}_{10}, \boldsymbol{x}_{12}$ and $\boldsymbol{x}_{35}$. Another random will visit samples $\boldsymbol{x}_{30}, \boldsymbol{x}_{11}, \boldsymbol{x}_2$ and $\boldsymbol{x}_0$. The same number of jumps for the two random walks is kept.

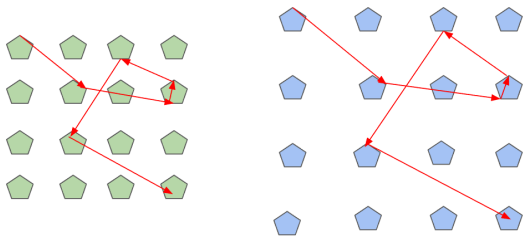

Figure A29: The lengths of the vectors of the same random walk can change as inter-cluster distances change.

Next, the lengths of the difference vectors between subsequent jumps are calculated. For example, from the first random walk we keep $||\boldsymbol{x}_{10} - \boldsymbol{x}_0||, ||\boldsymbol{x}_{12} - \boldsymbol{x}_{10}||$ and $||\boldsymbol{x}_{35} - \boldsymbol{x}_{12}||$ and from the second $||\boldsymbol{x}_{11} - \boldsymbol{x}_{30}||, ||\boldsymbol{x}_2 - \boldsymbol{x}_{11}||$ and $||\boldsymbol{x}_0 - \boldsymbol{x}_2||$. Here only 4 samples were used. But in the actual experiment we used N samples for each random walk and we repeat 100 times. Then if we calculate the histogram of these lengths for datasets of different levels of sparsity we obtain results such those of Fig. 4A. Now each histogram vector is fed to a regressor to predict a single value θ. A straightforward 1D CNN provides 0.99 accuracy of predicting the correct θ in this example. Calculating the random walks takes only a few seconds because the complexity of calculating the lengths is $\mathcal{O}$(N). The

histogram calculation for N of 1 million takes only 12 ms for 100 bins. Therefore, it does not delay execution. Finally, in order to understand why the lengths of these random walks become a signature of the underlying distribution please see Fig. A29.

A.14 On the stochasticity of Thetan Berserker

An algorithm is said to be stochastic if it incorporates randomness in its process or decision-making. This means that the algorithm's behavior or output may or not vary between executions, even when given the same input. More importantly stochastic algorithms use random variables or probabilistic components as part of their logic. Thetan Berseker (TB) is made to arrive at the similar conclusions given random orderings of the data samples. In addition, TB is employing randomness as part of a way of avoiding repeating the same ordering in Algorithm 2. This acts as an extra safety measure to ensure robustness.

A.15 Continuation of Large Simulation Experiment

In the following experiments, clustering was performed on different distributions. The Figures A31 to A45 are all the results obtained for various distributions. In the figures, the blue crosses indicate the ground truth centroid and the red crosses indicate the estimated centroids. The total number of clusters that are present is 300.

A.16 Varying Gaussian Distribution

Figures A31 to A35 highlight the performance of various clustering methods in predicting the centroids in varying gaussian distribution. The results indicate that TB, HDBSCAN, and Meanshift accurately identified the centroids, while KMeans++ and DBSCAN had minor inaccuracies, misidentying only a few centroids or adding some extra ones. Here, the parameters used were $\theta = 3.6$ for TB, $K = 300$ for KMeans++, $eps = 0.5$ and $min\_samples = 40$ for DBSCAN, $min\_samples = 40$ for HDBSCAN and $bandwidth = 2.6$ for Meanshift.

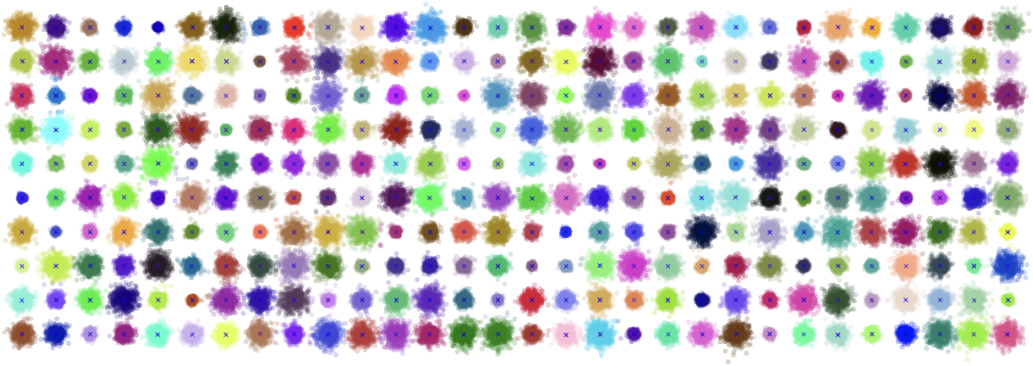

Figure A30: TB ($\theta = 3.6$)

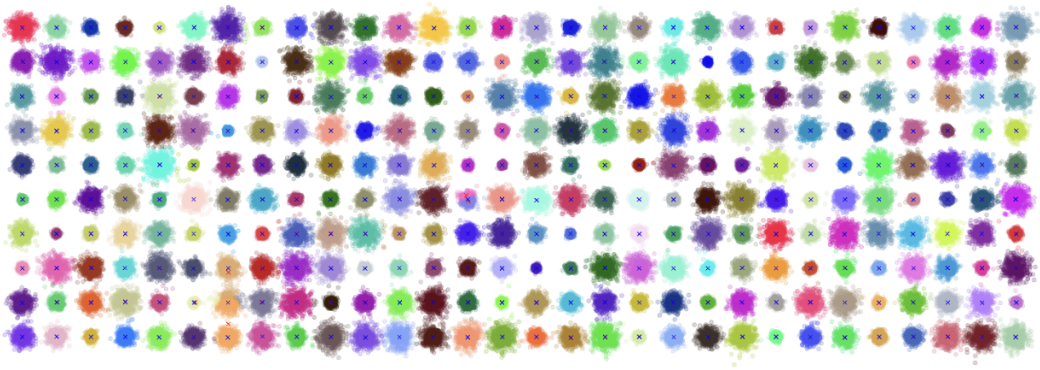

Figure A31: KMeans++ ($K = 300$)

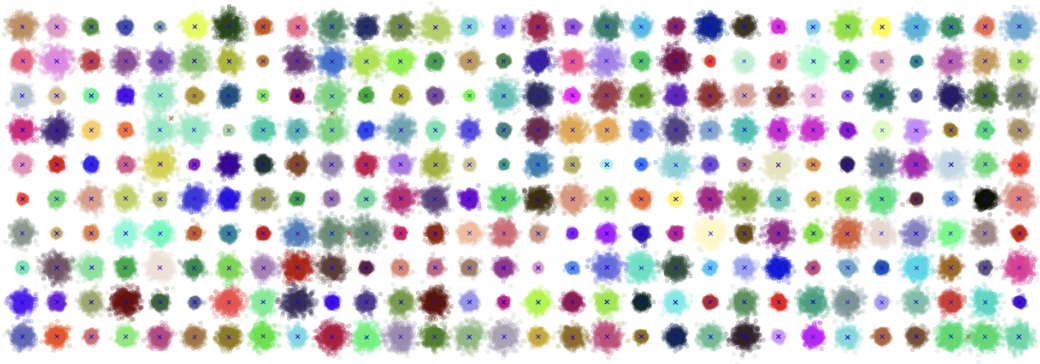

Figure A32: DBSCAN ($eps = 0.5, min\_samples = 40$)

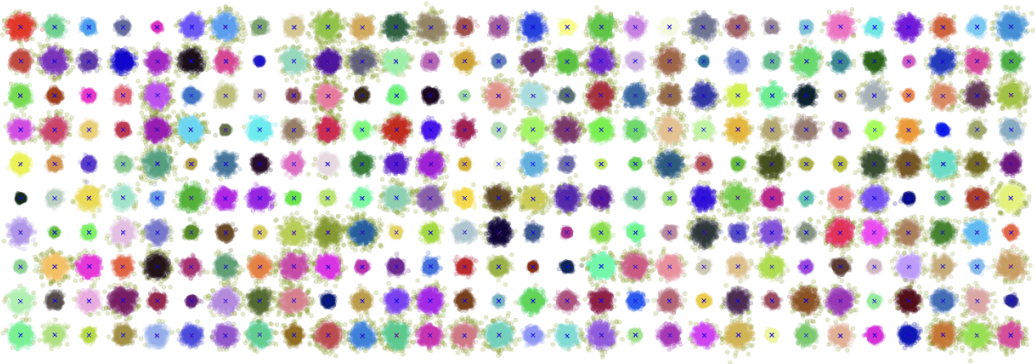

Figure A33: HDBSCAN ($min\_samples = 40$)

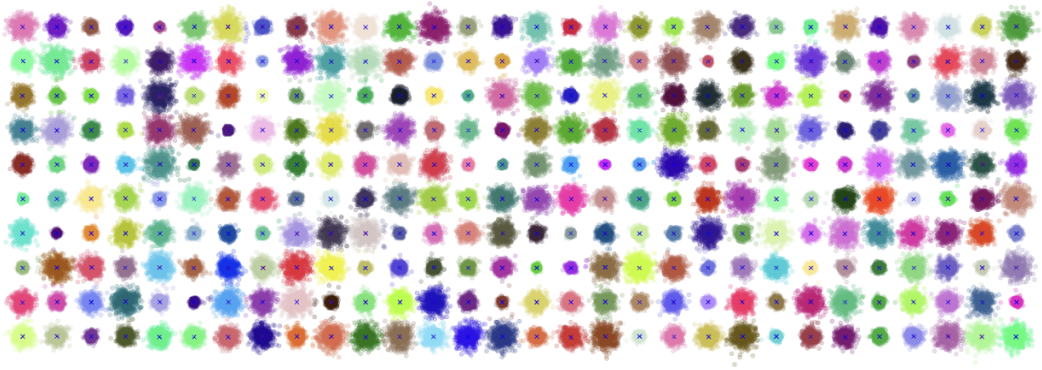

Figure A34: Meanshift ($bandwidth = 2.6$)

A.17 UNIFORM DISTRIBUTIONS

Figures A36 to A40 demonstrate the performance of various clustering methods in predicting the centroids in Uniform distribution. The results show that TB and DBSCAN accurately identified the centroids, whereas HDBSCAN and KMeans++ misidentified some of them. Meanshift, however, failed to correctly predict a significant number of centroids. The parameters used were $\theta = 5.6$ for TB, $K = 300$ for KMeans++, $eps = 0.5$ and $min\_samples = 40$ for DBSCAN, $min\_samples = 40$ for HDBSCAN and $bandwidth = 2.6$ for Meanshift.

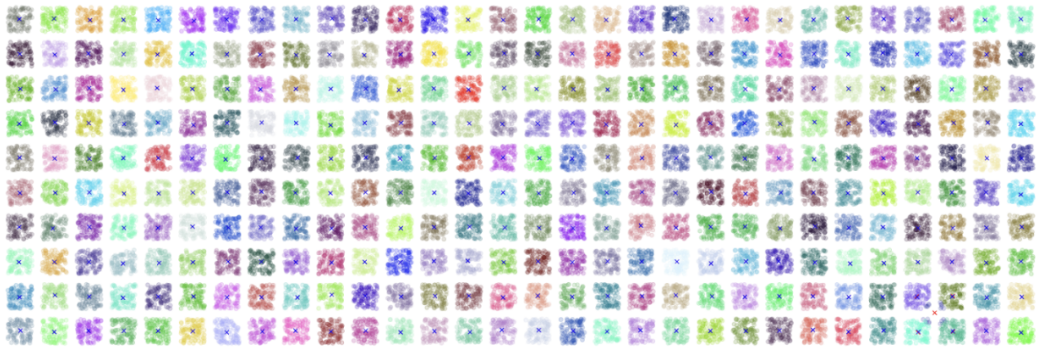

Figure A35: TB ($\theta = 5.6$)

Figure A36: KMeans++ ($K = 300$)

Figure A37: DBSCAN ($eps = 0.5, min\_samples = 40$)

Figure A38: HDBSCAN ($min\_samples = 40$)

Figure A39: MeanShift ($bandwidth = 2.6$)

A.18 Large Simulation Experiment on Varying Uniform Distributions

Figures A41 to A45 illustrate the performance of various clustering methods in predicting centroids in varying uniform distribution. The results indicate that TB, DBSCAN and HDBSCAN successfully identified the correct centroids, whereas KMeans++ and Meanshift misidentified some centroids. Similar to section A.17, the parameters used were $\theta = 5.6$ for TB, $K = 300$ for K-Means++, $eps = 0.5$ and $min\_samples = 40$ for DBSCAN, $min\_samples = 40$ for HDBSCAN and $bandwidth = 2.6$ for MeanShift.

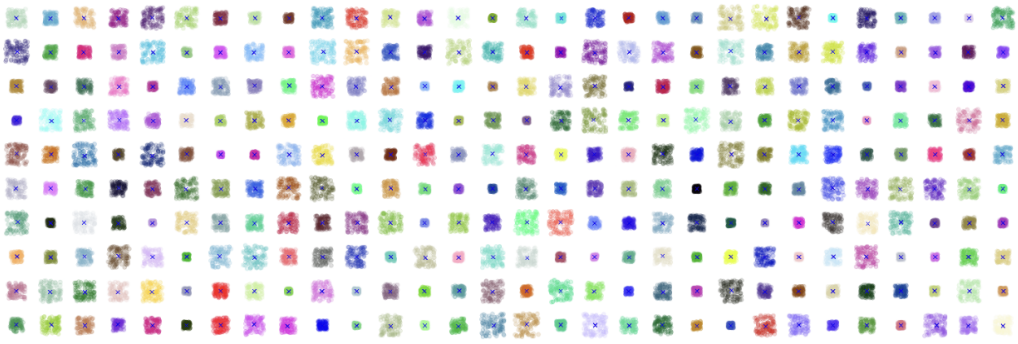

Figure A40: TB ($\theta = 5.6$)

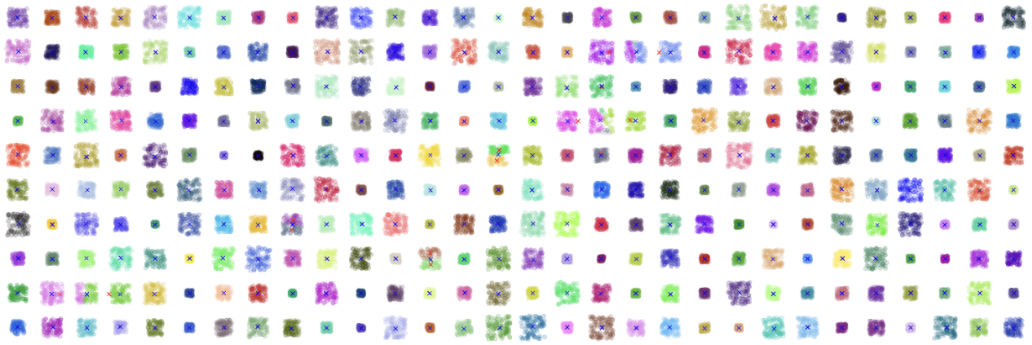

Figure A41: KMeans++ ($K = 300$)

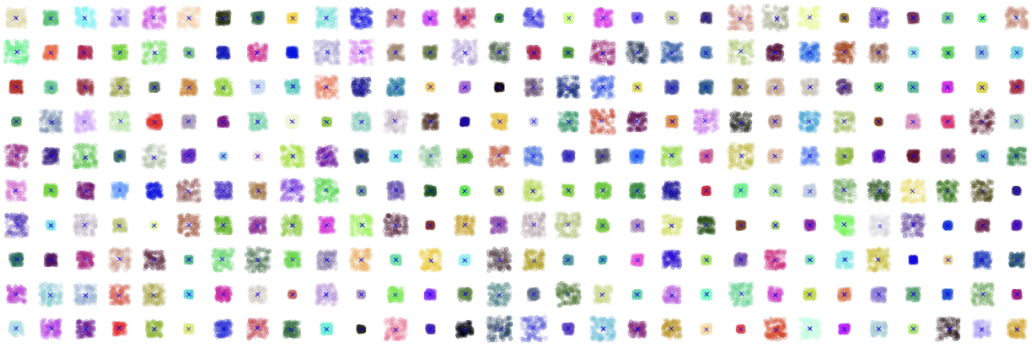

Figure A42: DBSCAN ($eps = 0.5, min\_samples = 40$)

Figure A43: HDBSCAN ($min\_samples = 40$)

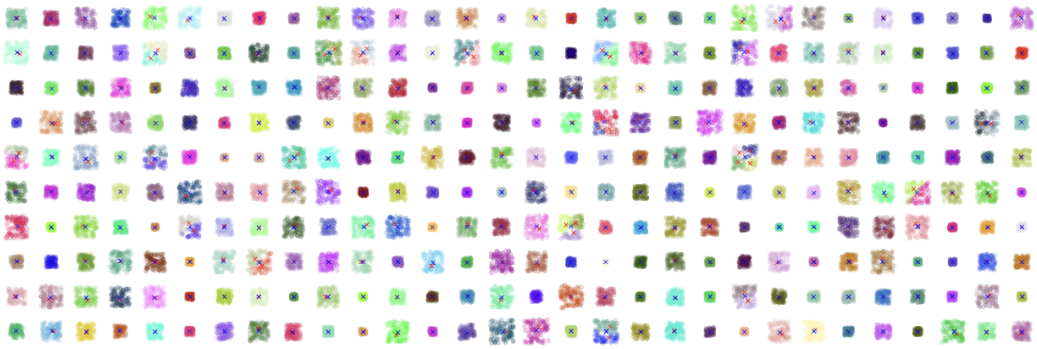

Figure A44: Meanshift ($bandwidth = 2.6$)

A.19 WHITE MATTER RECONSTRUCTION

Building on the discussion in 6.2, this section presents a processed slice from the T1-weighted images. The preprocessing steps and dimensions remain consistent with the earlier approach. Here, we used TB, KMeans and SLIC.
In the A45, A is the original T1 slice, B is the image obtained using TB with $\theta = 220$, C is the image obtained using KMeans with $K = 4$, D is the image obtained using SLIC with $n\_segments = 10$ and $compactness = 0.1$, E is TB with $\theta = 50$, F is KMeans with $K = 310$, and G is SLIC with $n\_segments = 100$ and $compactness = 0.1$.
TB does an excellent job in reconstructing the original T1 image for both values of θ, outperforming both KMeans and SLIC. Interestingly, KMeans with K=310 produces results very similar to TB with $\theta = 50$. However, for lower number of clusters KMeans is not performing too well. It reconstructs most of the image but with some loss of information. The number of clusters for KMeans was taken directly from TB's output. On the other hand, SLIC is not performing too well, with some loss of information in lower number of segments and the loss of information is high when the number of segments is 100.

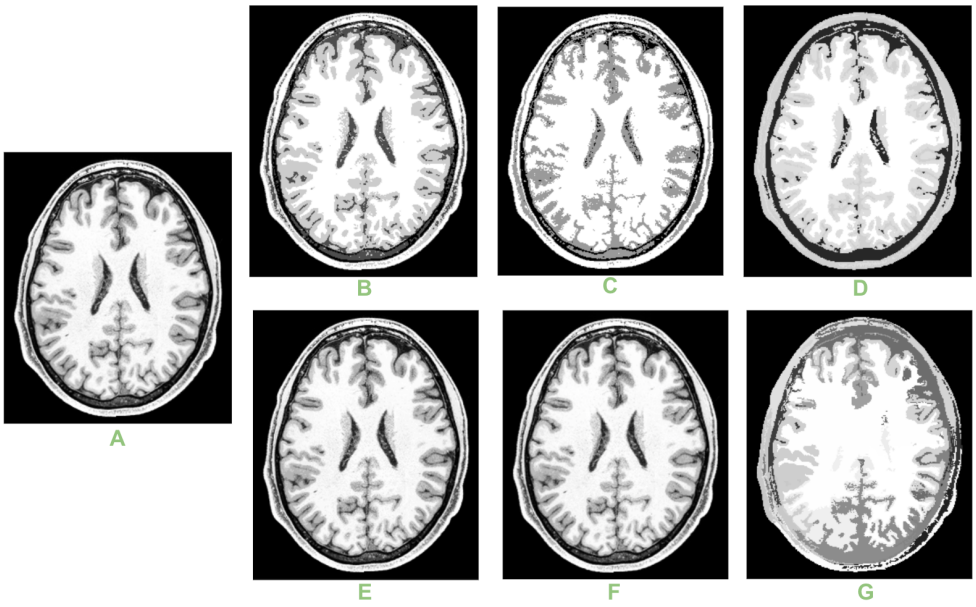

Figure A45: White Matter Reconstruction using Different Methods A) Original T1 Slice, B) TB (θ220), C) KMeans (K4), D) SLIC (n_segments 10), E) TB (θ50), F) KMeans (K310), G) SLIC (n_segments=100).

A.20 TEXT EMBEDDINGS

Here, TB was used for clustering in high-dimensional spaces, using text embeddings from the "PersonaHub FineWeb-Edu 4 Clustering 100k" dataset available on HuggingFace. The dataset comprises 100,000 samples, each represented by embeddings of dimensionality 1024. The performance of TB was benchmarked against KMeans++ and Marigold (Mortensen et al., 2023).
Table A5 highlights that TB requires less memory compared to both KMeans++ and Marigold when clustering the same number of clusters. In terms of execution time, TB outperforms KMeans++ but is marginally slower than Marigold. However, TB demonstrates superior clustering quality, achieving higher NMI and V-Measure scores than both KMeans++ and Marigold, while Marigold lags behind in these metrics.
For TB, the parameters used were $\theta = 0.48$, and the number of clusters derived from TB was applied to both KMeans++ and Marigold to ensure a fair comparison across methods.

Table A5: Comparisons between clustering algorithms for Text Embeddings

Method	Clusters	Memory (MB) ↓	Time (s) ↓	NMI ↑	V-Measure ↑
TB	5641	**156**	85.9667	**0.5252**	**0.5252**
KMeans++	5641	166	89.2508	0.5239	0.5239
Marigold	5641	312	**82.2857**	0.5130	0.5130

A.21 1D Signal Denoising

Here, we demonstrate the use of TB in denoising 1-dimensional signals. For this purpose, a synthetic signal which was a sine wave along with random gaussian noise was used. A sliding window of 98 was used on the signal which becomes the feature space. The signal was then normalized by scaling the data. Fig A46, shows the results obtained after TB was used to denoise the signal. The reconstructed sine wave is near identical to the clean noise-free sine wave. The parameters that were used is θ=174.

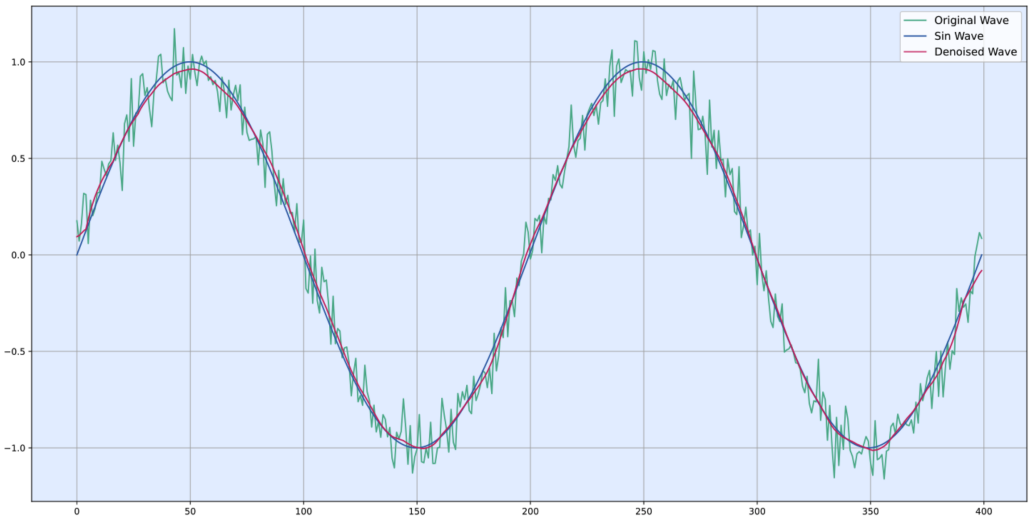

Figure A46: A sine wave denoised using TB clustering.

A.22 Summary of contributions

a) Remarkably fast clustering algorithm guaranteed to be between $\mathcal{O}(n)$ and $\mathcal{O}(n^2)$.

b) Exceptionally memory efficient with best and worst case at $\mathcal{O}(n)$.

c) Outperforming in 30 experiments across datasets, dimensions and evaluation metrics.

d) Highly interpretable consisting primarily of two compact algorithms.

e) Has only one hyper-parameter.

f) Can be used as standalone or as a way to improve the speed and conditioning of other known methods.

g) Widely applicable. Examples shown in real signal, image and text processing.